This work studies propagation of different SH-SAWs treating various configurations using the cubic crystals Bi12SiO20 and Bi12GeO20, which possess strong piezoelectric effect. Possible cuts for the wave propagation are treated when an even-order symmetry axis of a crystal is perpendicular to the sagittal plane, and when some analytical solutions can be obtained studying propagation direction [101] in the crystals. Calculations of the phase velocity and the CEMC versus the layer thickness were carried out. Numerical results on propagation of the seven-partial Love type waves were also introduced for different electrical boundary conditions: metallized and non-metallized surfaces. Also, new dispersive SAW possessing single mode was discovered concerning direction [101] in various layered systems consisting of the cubic crystals. It is thought that the obtained results can be also useful in the application of inter-digital transducers for excitation of different SAWs in structural health monitoring. In addition, a theoretical study of three-layer structures consisting of widely-used weak piezoelectrics (GaAs/GaP/GaAs and GaAs/GaP/ZnTe) was also carried out.

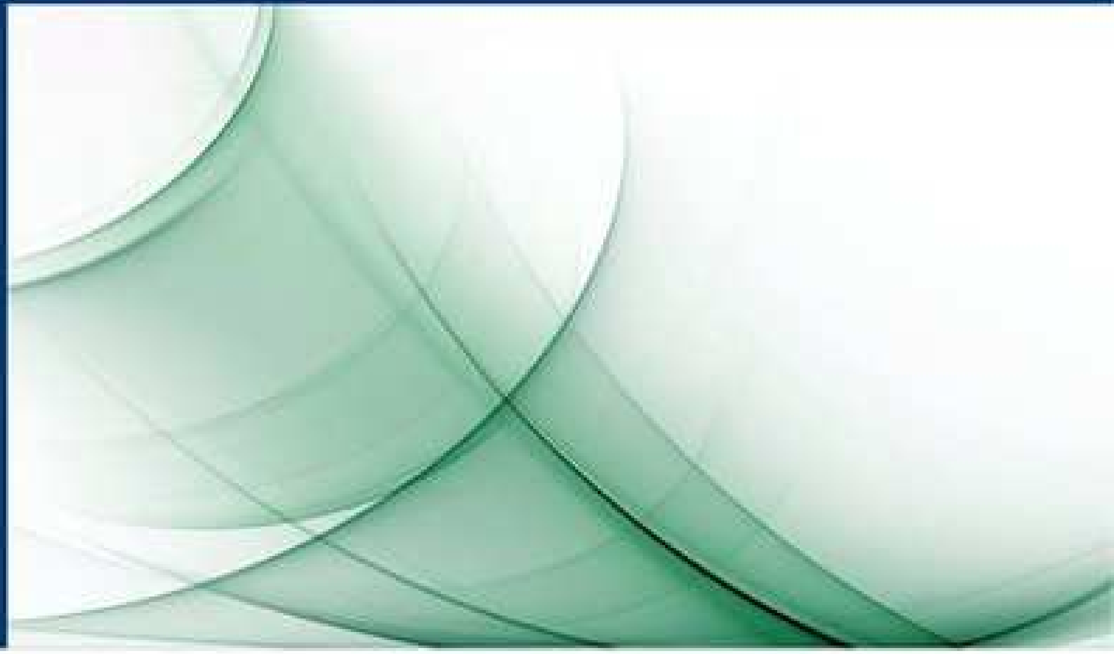

Aleksey Zakharenko

ALEKSEY ANATOLIEVICH ZAKHARENKO International Institute of Zakharenko Waves (IIZWs, aazaaz@inbox.ru) Education: 1998–Diploma Engineer-Physicist (MSc) Krasnoyarsk State University, Krasnoyarsk, Russia 2008–Certified Interior Designer (AutoCAD, 3ds max) Business School INOPROF, Krasnoyarsk, Russia. Research Experience: Creator of the IIZWs

9 783843 375238 978-3-8433-7523-8

Aleksey Zakharenko

Dispersive SAWs in Layered Systems Consisting of Cubic Piezoelectrics

New Dispersive Shear-Horizontal Waves and Love Type Waves in Layered Systems Consisting of Cubic Piezoelectrics

LAP LAMBERT Academic Publishing

This work has been fulfilled
within the International Institute of Zakharenko Waves by
ALEKSEY ANATOLIEVICH ZAKHARENKO
(E-mail: aazaaz@inbox.ru)

LAP LAMBERT Academic Publishing GmbH & Co. KG
Dudweiler Landstrasse 99 D - 66123 Saarbruecken
Phone: +49 681 3720-310 Fax: +49 681 3720 -3109
info@lap-publishing.com http://www.lap-publishing.com

Saarbruecken – Krasnoyarsk, 2010

PREFACE

This book theoretically studies propagation of different shear-horizontal acoustic waves in two-layer systems. Various configurations are treated using the cubic crystals $Bi_{12}SiO_{20}$ and $Bi_{12}GeO_{20}$ which possess strong piezoelectric effect. Possible cuts for the wave propagation are treated when an even-order symmetry axis is perpendicular to the sagittal plane, and when some analytical solutions can be obtained studying propagation direction [101] in the crystals. Calculations of the phase velocity V_{ph} and the static coefficient of electromechanical coupling K^2 versus the layer thickness were carried out. The calculation of the phase velocity V_{ph} can be useful for finding new shear-horizontal surface acoustic waves (SH-SAWs). Numerical results on propagation of the seven-partial Love type waves were also introduced for different electrical boundary conditions: metallized and non-metallized surfaces. Also, new dispersive SAW possessing single mode confined in suitable V_{ph}-range was discovered concerning direction [101] in various layered systems consisting of the cubic crystals. It was also found that speeds of non-dispersive surface and interfacial waves are possible limit speeds for the new dispersive SH-SAWs in the cases of the wavenumber $k \to 0$ and $k \to \infty$. However, the V_{ph} for some modes of the new dispersive waves can approach other limit speeds for a large value of the wavenumber k. The new SH-SAW existence broadens choice of piezoelectric materials which can be used in SH-SAW technical devices. It is thought that the obtained results can be also useful in the application of inter-digital transducers for excitation of different SAWs in structural health monitoring. In addition, theoretical study of three-layer structures consisting of widely-used weak piezoelectrics (GaAs/GaP/GaAs and GaAs/GaP/ZnTe) was carried out concerning any possibility to numerically find the new dispersive SH-SAWs.

PACS: 51.40.+p, 62.65.+k, 68.35.Gy, 68.35.Iv, 68.60.Bs, 74.25.Ld

Keywords: piezoelectric cubic crystals, strong piezoelectric coupling, new SH-SAWs, Love type waves.

COMMENTS BY THE AUTHOR

This book describes the theoretical work carried out for the International Institute of Zakharenko Waves (IIZWs) as an additional work to the PhD-thesis by the author: Aleksey Anatolievich Zakharenko, corresponding address is 660037, Krasnoyarsk-37, 17701, Krasnoyarsk, Russia (E-mail: aazaaz@inbox.ru). It is thought that this book can be interesting for researchers and students who deal with piezoelectrics, piezomagnetics, and layered systems consisting of them. It is also thought that it can represent an interest for those who cope with piezoelectromagnetics. Indeed, knowledge of properties of cubic piezoelectrics is beneficial to design of smart devices, sensors, actuators, as well as applications in non-destructive testing. Also, the obtained results in this book can allow one to choose apt materials to constitute piezomagnetic/piezoelectric laminate composites in the microwave technology. It is well-known that innovative smart materials are also created for the aerospace industry.

The International Institute of Zakharenko Waves (IIZWs) was recently created for support of different Zakharenko waves, as well as for monitoring the non-dispersive Zakharenko type waves in complex systems such as layered and quantum systems. Indeed, any complex system in which dispersive waves can propagate is of a great interest for the IIZWs. The well-known examples of dispersive waves are dispersive Rayleigh and Bleustein-Gulyaev type waves as well as Love and Lamb type waves. There are currently more than twenty papers relevant to the IIZWs. The International Institute of Zakharenko Waves also studies different dispersive and non-dispersive waves both theoretically and experimentally, including different applications of the waves for signal processing (filters, sensors, etc.) and the structural health monitoring. Note that one can financially support the research of the International Institute of Zakharenko Waves, using the following bank account: Beneficiary's Bank is Krasnoyarsk Branch of National Bank TRUST, c/a № 30301978300450000038 with Moscow Branch of National Bank TRUST, Moscow, Russia, SWIFT: MENARU2PMOS, via correspondent account no. 0103886388 with OST-West HandelsBank AG, Frankfurt-am-Main, Germany (SWIFT: OWHBDEFF). Beneficiary customer: Aleksey Zakharenko with Beneficiary's account: 42301978600380000278 .

It is worth noting that the International Institute of Zakharenko waves possessively takes all the planets and smaller natural space bodies in the space outside the Solar System to develop both the IIZWs and the planets concerning economics, ecology, and population. Also, it is thought that this is necessary in order to exclude any sale of the planets and their surfaces by any human or other. This activity of the IIZWs was also created due to a problem to find a spot for the IIZWs on Earth. Note that the single person, namely Mr. Dennis Hope from the United States possesses the planets in the Solar System (but Earth) who sells surfaces of the planets to individuals. It is also noted that only about 500 planets orbiting stars can be currently observed in Star Systems which are situated relatively near the Solar System. This does not mean that only 500 planets exist outside the Solar System we can observe. It is expected that in average ten planets can orbit each star of enormous number of Star System in our Universe. It is thought that our Universe can accumulate more than 10^{999} stars.

Aleksey A. Zakharenko

Krasnoyarsk, Russia, 2010

TABLE OF CONTENTS: **PAGE**

List of Tables:

List of Figures: **PAGE**

INTRODUCTION

It is well-known that there are two basic polarization types for surface acoustic waves (SAWs) in acoustics of solids such as the wave polarization in the sagittal plane and the polarization perpendicular to the sagittal plane. The sagittal plane is formed by the directional vector **M** and the vector **N** being the normal to both the free surface and interface shown in figure 1 along with the coordinate system for the layered system, consisting of a thin film (layer) on a substrate (half-space). The surface Rayleigh waves possessing hybridization of the displacement components U_1 and U_3 along the x_1- and x_3-axes are polarized in the sagittal plane. These waves were originally discovered in 1885 by Lord Rayleigh [1]. Note that Lord Rayleigh has studied isotropic mono-materials, namely the case of the layer thickness $h = 0$ in figure 1. It is thought that the SAW simplest example concerning the polarization perpendicular to the sagittal plane is the Love wave [2] propagating in layered systems, consisting of two isotropic materials. Note that there is the following existence condition for Love waves: the speed $V_{SH} = (C_{44}/\rho)^{1/2}$ of the bulk shear-horizontal (SH) wave for a substrate should be higher than that for a layer, where C_{44} and ρ are the shear elastic constant and material density, respectively. For the Love (type) waves, the displacement component U_2 along the x_2-axis for a substrate is coupled with the component U_2 for a layer at the layer-substrate interface. Therefore, they are hybridized due to their co-influence. The Love type wave (LTW) becomes the bulk SH-wave for zero layer thickness and cannot exist in homogeneous monocrystals.

SAWs with the Love-wave polarization can also exist in inhomogeneous media such as piezoelectric monocrystals. They were first discovered by Bleustein and Gulyaev simultaneously in the late 1960s [3, 4] studying transversely-isotropic piezoelectrics of class 6 mm. The surface Bleustein-Gulyaev type waves (BGTWs) are treated as the weakly-nonhomogeneous SAWs. They can exist only on certain cuts and propagate in certain directions of piezoelectric monocrystals characterized by coupling between the elastic displacement component U_2 and electrical potential $U_4 = \varphi$, where φ is electrostatically defined from the electrical field $E_j = \partial\varphi/\partial x_j$ with the index j = 1, 2, 3. Hence, it is thought that there must be a coupling of at least two displacement components in the SAW simplest cases.

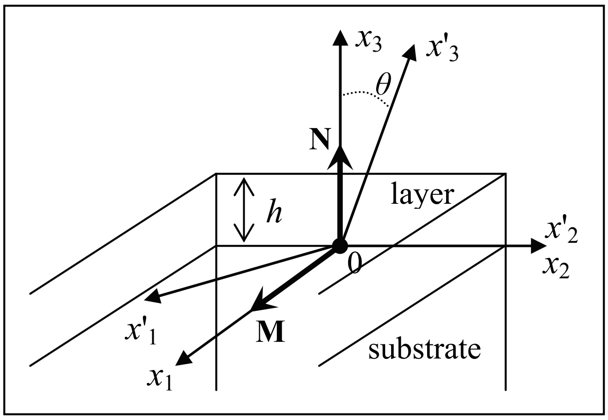

Figure 1. The right coordinate system with the directional vector **M**||[100] and the vector-normal **N** for the layered structure consisting of a layer on a substrate, where h is the layer thickness

Dispersive Rayleigh type waves (RTWs) can propagate in the layered systems shown in figure 1 in which the LTWs can also co-exist. In layered systems consisting of two piezoelectric materials, the “pure” RTWs are coupled with the electrical potential when LTWs represent pure mechanical waves and vice versa, according to Refs. [5, 6, 7]. See also the famous book [8] describing applications of the RTW, LTW, and BGTW. Recently, interest is growing in the study of propagation of dispersive BGTWs in various layered structures (for example see Ref. [9]) because the application of layered piezoelectric structures can significantly reduce the penetration depth, which is 10 – 100 times larger than the wavelength λ for the surface BG-waves in monocrystals. It is thought that the single mode of dispersive BGTWs can be treated as the LTW lowest-order mode, which represents the LTW first type. It is also thought that the LTW higher-order modes represent the LTW second type in order to have an analogy with the dispersive RTWs, of which the first (lowest-order mode) and second types are separately studied.

In general, propagation of the dispersive and non-dispersive BGTWs is studied in the transversely-isotropic materials. Moreover, one of the BG-wave discoverers stated in Ref. [10] published in 2005 that the SAWs cannot exist in piezoelectric cubic monocrystals. Indeed, such surface waves were not found in Ref. [11] studying cubic piezocrystals of class 23 in propagation direction (001) [100]. It is noted that in 1966, Kaganov and Sklovskaya [12] reported a possible existence of new surface waves coupled with the electrical potential in piezoelectric cubic monocrystals in addition to the purely mechanical surface Rayleigh waves. Treating the case of elastically-isotropic medium with the non-zero piezoelectric constants $e_{14} = e_{25} = e_{36}$, they in Ref. [12] have found that the phase velocity V_{ph} of the new (additional) surface wave is higher than $3^{1/2}c_t/2$ and lower than c_t, according to the paper text (the abstract in Ref. [12] was incorrectly written) where c_t represents the bulk shear wave velocity uncoupled with the electrical potential. In addition, they did not state that such new SAWs can propagate when the wave propagation direction is perpendicular to an even-order symmetry axis of a piezoelectric crystal. Indeed, utilization of cubic piezoelectrics in addition to the transversely-isotropic materials can broaden a list of suitable materials and represents an interest in engineering and design of SAW devices (filters, dispersive delay lines, etc.).

According to Ref. [13] by Al'shits and Lyubimov, the BG-wave existence in cubic piezocrystals of classes $\bar{4}3$ m and 23 strongly depends on the piezoelectric constants and dielectric constant ε. Ref. [13] has discussed that existence sectors of the BG-waves being about $\pi/4$, when there is rotation around the axis directed along an even-order symmetry axis, can be significantly broadened using crystals with small dielectric constants. For the limit case of $\varepsilon \to 0$ requiring small piezoelectric constants, the BG-waves can exist in any such propagation direction, except the exceptional angles 0, $\pi/2$, π, …, where the single-partial exceptional bulk waves of first type can exist representing the boundaries of such SAW existence sectors. Also, only the exceptional bulk waves can exist in piezoelectric cubic monocrystals possessing a very large dielectric constant $\varepsilon \to \infty$ [13] for the second limit case. They also noted that there is an analogy of existence of exceptional bulk waves in optics, where surface optic waves can be converted to bulk waves for some frequencies and propagation directions. Indeed, different electrical boundary conditions (for example, the surface metallization) can also alter the existence sectors of the BG-waves. It is thought that the interesting case of $\varepsilon \to \infty$ can be realized due to recent discovery of the giant dielectric effect found in the cubic perovskite-related materials $CdCu_3Ti_4O_{12}$ and $CaCu_3Ti_4O_{12}$ [14]. The latter has a tremendously high dielectric constant $\varepsilon_s \sim 10^4$ at room temperatures. One of the most commonly used dielectric materials is silicon nitride with $\varepsilon_s \sim 7$. Materials with large static dielectric constants $\varepsilon_s > 7$ are generally referred to as high-dielectric constant materials and are used in memory devices being highly called for the microelectronics industry. That is due to the fact that acting as a scaling factor, the static dielectric constant ε_s ultimately determines the miniaturization level.

The recent review paper [15] by Yamaguchi focused on early days of research about SH type acoustic waves. For instance, it was discussed in Ref. [15] that the surface skimming bulk waves (SSBWs) are closely related to the other SAWs known as the Bleustein-Gulyaev-Shimizu waves (BGSWs) on rotated *Y*-cuts of quartz, namely the SSBW velocities substantially coincide with those of BGSW. Also, some types of SH-SAWs in solids can be found in the famous review paper [16] by Gulyaev, see also the famous book [17] on wave phenomena in inhomogeneous media. A possible existence of two new types of SH-SAWs propagating in layered systems, consisting of a layer on a substrate, was recently introduced in Ref. [18], of which one can be used in addition to the Love type waves. Ref. [18] also shows the existence possibility of the supersonic three-partial Love type waves (LTW3) where the velocity equivalents for both layer and substrate, instead of the bulk SH-waves, should be analyzed for the wave existence condition. It is noted that the velocity equivalent is always lower that the bulk SH-wave speed for anisotropic materials. It is thought that these velocity equivalents can be also called the exceptional bulk waves. This paper studies different dispersive and non-dispersive waves with the

Love-wave polarization. The following section contains thermodynamic description of the material constants in the linear case. Also, the following section provides evolution of the piezoelectric constants caused by changes in the wave propagation directions when the elastic and dielectric constants are not changed.

CHAPTER I. Material Properties

Piezoelectric ceramics are used in a variety of commercial applications due to their electromechanical nature displaying both a direct effect (generating effect) in which an electrical charge is generated by a mechanical stress, and the converse effect (motor effect) in which an electrical field produces a mechanical displacement. Note that piezoelectricity from the Greek word "piezo" means pressure electricity. Various solid-state or polymeric materials with piezoelectric characteristics are being applied to a variety of transducers and sensors, which include hydrophones, sonar, accelerometers, power supplies, ultrasonic motors, transformers, micropositioners, filters, robotic muscles, medical ultrasound, etc. Currently, piezoelectric ceramics are the most widely used materials, because they comparatively show the highest generative forces, accurate displacements, and best high frequency capabilities. When an AC voltage is applied to a sample piezoelectric material, it will cause vibrations and thus generate mechanical waves at the same frequency of the input AC field. Similarly, it would sense the input mechanical vibrations and produce the proportional charge at the matching frequency of the mechanical input. Quartz is a well-known single-crystal material, depicting such piezoelectric effects. The pioneer work by W.G. Cady [19] concerning applications of Quartz piezoelectric crystals attracted attention to the utilization of piezoelectric crystals in various technical devices. The famous review papers [20, 21] by W.P. Mason describe many applications of piezoelectrics over the last century, including different SAW technical devices.

According to the classical works [22, 23], the thermodynamic potentials derive the equations of piezoelectric medium. In order to describe thermoelectroelastic interactions in piezoelectric crystals, eight thermodynamic potentials are currently used, in which energetic terms are included and are coupled with elastic (stress τ_{ij} or strain η_{ij}), electric (electrical field E_i or electrical induction D_i) and thermal (temperature T or disorder value called entropy S) sub-systems [23]. General equations for adiabatic rather than isothermal conditions may be obtained using the thermodynamic potential (electrical enthalpy $H_{el}{}^{a}$) given by the following expression:

$$H_{el}^{a} = \tau_{ij}\eta_{ij} - D_m E_m - T_k S_k \tag{1}$$

It is thought that it is convenient to naturally take the mechanical strain tensor η_{ij} as an independent thermodynamic mechanical variable, because the wavelength of propagating acoustic waves is significantly smaller than line sizes of a sample crystal, and crystal vibrations as a whole can be neglected (mechanically-shorting condition). Also, the electrical field E_m is taken as a thermodynamic electrical variable, because the piezoactive propagation directions can exist in piezoelectric materials where the electrical potential is coupled with propagating elastic waves. The perfect differential of equation (1) is then written in the following way:

$$\mathrm{d}H_{el}^{a} = \tau_{ij}\mathrm{d}\eta_{ij} - D_m \mathrm{d}E_m - T_k \mathrm{d}S_k \tag{2}$$

Treating adiabatic processes with the constant entropy (S = const giving dS = 0) and leaving only linear terms, it is possible to write a Taylor series for the electrical enthalpy $H_{el}{}^{a}(\eta_{ij}, E_m, S)$ relative to an equilibrium condition $H_{el}{}^{a}(0, 0, S_0)$:

$$H_{el}^{a}(\eta_{ij}, E_m, S) - H_{el}^{a}(0,0,S_0) = \frac{1}{2}C_{ijkl}^{E}\eta_{ij}\eta_{kl} - e_{mij}\eta_{ij}E_m - \frac{1}{2}\varepsilon_{mn}^{\eta}E_m E_n \tag{3}$$

With vibrating piezoelectric elements there is usually negligible heat interchange, and the adiabatic equations hold. Using equation (3), it is possible to write "mechanical" and "electrical" equations for the treated linear case. With the stress and electrical field as the independent variables, the equations are written as follows:

$$\tau_{ij} = \left(\frac{\partial H_{el}^{a}}{\partial \eta_{ij}}\right)_{E,S} = C_{ijkl}^{E}\eta_{kl} - e_{ijm}E_m \tag{4}$$

$$D_m = -\left(\frac{\partial H_{el}^a}{\partial E_m}\right)_{\eta,S} = \varepsilon_{mn}^{\eta} E_n + e_{mij}\eta_{ij} \tag{5}$$

The elastic constants C_{ijkl}, being components of the elastic stiffness tensor, relate two second-order symmetric tensors representing fourth-order tensors from equation (4) for linear elasticity with piezoelectric term:

$$C_{ijkl}^{E,S} = \left(\frac{\partial^2 H_{el}^a}{\partial \eta_{ij}\partial \eta_{kl}}\right)_{E,S} = \left(\frac{\partial \tau_{ij}}{\partial \eta_{kl}}\right)_{E,S} \tag{6}$$

The piezoelectric constants e_{mij} relate second-order symmetric tensors to vectors, and therefore they are third-order tensors, using equations (4) and (5):

$$e_{mij}^S = e_{ijm}^S = -\left(\frac{\partial^2 H_{el}^a}{\partial \eta_{ij}\partial E_m}\right)_S = -\left(\frac{\partial \tau_{ij}}{\partial E_m}\right)_{\eta,S} = \left(\frac{\partial D_m}{\partial \eta_{ij}}\right)_{E,S} \tag{7}$$

The dielectric constants ε_{mn}, also called dielectric permittivity, relate two vectors, and therefore represent second-order tensors. Using equation (5), they are defined as follows:

$$\varepsilon_{mn}^{\eta,S} = -\left(\frac{\partial^2 H_{el}^a}{\partial E_m \partial E_n}\right)_{\eta,S} = \left(\frac{\partial D_m}{\partial E_n}\right)_{\eta,S} \tag{8}$$

Accounting the fact, such as the sound velocity V in a crystal is very small compared with the light velocity c, allows usage of the quasi-electrostatic approximation

$$\mathrm{rot}\mathbf{E} = 0 \text{ or } E_m = -\frac{\partial \varphi}{\partial x_m} \tag{9}$$

with φ and x_m being the electrical potential and current rectangular coordinates of a material point, respectively. On the other hand, the electrical induction D_m must satisfy the Maxwell equation for a non-conducting medium

$$\mathrm{div}\mathbf{D} = \frac{\partial D_m}{\partial x_m} = 0 \tag{10}$$

Note that equation (8) gives the well-known relationship $D_m = \varepsilon_{mn}E_n$ between the electrical induction D_m and the electrical field E_n.

The corresponding material tensors in equations from (6) to (8), being invariant relative to the crystallographic group of symmetry, are described in the famous book [24] by J.F. Nye. Note that crystal symmetry is coupled with symmetry of physical properties of a crystal. The fundamental postulate of crystallophysics known as the Neumann principle (for example see Ref. [24]) states the following: "Symmetry elements of any crystal physical property should include symmetry elements of crystal point group". Each crystal point group has its own set of independent components of material tensors. For instance, piezoelectric cubic crystal $Bi_{12}SiO_{20}$ (class 23) has the following independent material constants (in the Voigt notation): $C_{11} = C_{22} = C_{33}$, $C_{12} = C_{13} = C_{23}$, $C_{44} = C_{55} = C_{66}$; $e_{14} = e_{25} = e_{36}$ and $\varepsilon_{11} = \varepsilon_{22} = \varepsilon_{33}$ in addition to the material density ρ. Material constants for cubic crystals $Bi_{12}SiO_{20}$ and $Bi_{12}GeO_{20}$ can be written following Ref. [25]. For $Bi_{12}SiO_{20}$ there are the following material constants: $\rho = 9070$ [kg/m^3]; $C_{11} = 12.962\times10^{10}$ [N/m^2], $C_{44} = 2.451\times10^{10}$ [N/m^2], and $C_{12} = 2.985\times10^{10}$ [N/m^2]; $e_{14} = 1.122$ [C/m^2]; $\varepsilon_{11}/\varepsilon_0 = 41.1$ where ε_0 is the free space dielectric permittivity ($\varepsilon_0 = 8.854\times10^{-12}$ [F/m]). For $Bi_{12}GeO_{20}$ there are: $\rho = 9200$ [kg/m^3]; $C_{11} = 12.852\times10^{10}$ [N/m^2], $C_{44} = 2.562\times10^{10}$ [N/m^2], and $C_{12} = 2.934\times10^{10}$ [N/m^2]; $e_{14} = 0.983$ [C/m^2]; $\varepsilon_{11} = 3.336\times10^{-10}$ [F/m]. Transformations of any tensor component from the original coordinate system ($x_1x_2x_3$ in figure 1) to the "work" coordinate system ($x'_1x'_2x'_3$ in figure 1) are perfectly described in the excellent books [8, 24]. Transformed components ε_{ij} of the dielectric permittivity tensor can be calculated using given original components ε_{mn} and corresponding components a_{im} and a_{jn} of the transformation matrix:

$$\varepsilon_{ij} = a_{im} a_{jn} \varepsilon_{mn} \tag{11}$$

Analogically, components of the piezoelectric and elastic tensors after transformations are obtained with the following formulae:

$$e_{ijk} = a_{im} a_{jn} a_{kp} e_{mnp} \tag{12}$$

$$C_{ijkl} = a_{im} a_{jn} a_{kp} a_{lq} C_{mnpq} \tag{13}$$

The crystallographic coordinates (X, Y, Z) coincide with the original coordinates (x_1, x_2, x_3) in figure 1. Acoustic waves propagate along the x'_1-axis in the work coordinate system (x'_1, x'_2, x'_3) obtained by rotation around the x'_2-axis, which must be directed along an even-order symmetry axis of a studied crystal. The direction of the cut normal is also changed with the Euler angles (0°; θ; 0°). Therefore, the coordinate transformations read:

$$a_{\mu\nu}^{(\theta)} = \begin{pmatrix} \cos\theta & 0 & -\sin\theta \\ 0 & 1 & 0 \\ \sin\theta & 0 & \cos\theta \end{pmatrix} \tag{14}$$

For instance, the components of the transformation matrix (14) for the angle $\theta = \pi/4$ are as follows:

$$a_{\mu\nu}^{(\pi/4)} = \begin{pmatrix} 1/\sqrt{2} & 0 & -1/\sqrt{2} \\ 0 & 1 & 0 \\ 1/\sqrt{2} & 0 & 1/\sqrt{2} \end{pmatrix} \tag{15}$$

For piezoelectric cubic crystals, the transformations keep the material constants $C_{44}(\theta)$ and $\varepsilon_{11}(\theta)$, but the piezoelectric constants $e_{ij}(\theta)$ are changed as shown in figure 2 for the cubic crystal $Bi_{12}SiO_{20}$. That conveniently allows study of piezoelectric properties of crystals.

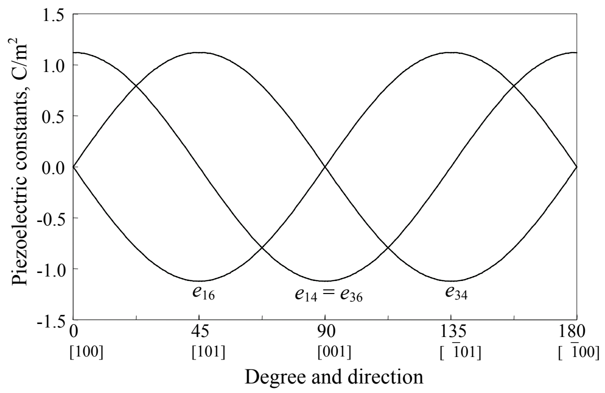

Figure 2. The dependence of the piezoelectric constants $e_{14} = e_{36}$, e_{16}, and e_{34} on the propagation directions with the Euler angles $\{0^o, \theta, 0^o\}$ for the cubic crystal $Bi_{12}SiO_{20}$

This book describes wave propagation with the Love-wave polarization in various layered systems consisting of cubic crystals $Bi_{12}SiO_{20}$ and $Bi_{12}GeO_{20}$ with strong piezoelectric effect, when the propagation directions are perpendicular to the crystal second-order symmetry axis. Particularly, it will be shown below that the surface Bleustein-Gulyaev waves cannot exist in piezoelectric cubic crystals, supplementing Gulyaev's opinion written in Ref. [10] concerning the surface waves in the crystals mentioned in the previous section. The following section describes theory of wave propagation in different cuts and propagation directions, and the fourth and fifth sections provide boundary-condition determinants for finding the phase velocity V_{ph} of SH-waves in piezoelectric monocrystals and layered systems. The sixth section adds some obtained results of numerical investigations concerning the V_{ph} behavior in a set of configurations for complete understanding of the problem.

CHAPTER II. Theory of Propagating Waves

The equation of motion of an elastic medium is written as follows [6, 7]:

$$\rho \frac{\partial^2 U_i}{\partial t^2} = \frac{\partial \tau_{ik}}{\partial x_k} \tag{16}$$

which represents the governing equation of stress equilibrium, where ρ denotes the material density. U_i and τ_{ij} are the mechanical displacement components and components of the stress tensor thermodynamically defined in equation (4), respectively. In equation (14), t and x_k are time and the real space vector components $\mathbf{r} \to \{x_1, x_2, x_3\}$ using the rectangular co-ordinate system. Substituting equations (4) and (5) into (16) and (10), respectively, and accounting expression (9) for the electrical field, one can write the coupled equations of motion for a piezoelectric medium in the common form:

$$\begin{aligned} \rho \frac{\partial^2 U_i}{\partial t^2} &= C_{ijkl} \frac{\partial^2 U_l}{\partial x_j \partial x_k} + e_{kij} \frac{\partial^2 U_4}{\partial x_j \partial x_k} \\ 0 &= e_{ijk} \frac{\partial^2 U_k}{\partial x_i \partial x_j} - \varepsilon_{ij} \frac{\partial^2 U_4}{\partial x_i \partial x_j} \end{aligned} \tag{17}$$

where the component U_4 represents the electrical potential φ. Solutions of homogeneous partial differential equations (17) of the second order can be found in the following form of plane wave:

$$U_i = U_i^0 \exp[\mathrm{j}(\mathbf{kr} - \omega t)] \tag{18}$$

where the index i runs from 1 to 4, and U_i^0 is an initial amplitude. $\mathrm{j} = (-1)^{1/2}$ and **kr** denote the imaginary unity and scalar multiplication of two vectors, respectively. In equation (18), ω and **k** are the angular frequency and wavevector with the following components: $\{k_1, k_2, k_3\} = k\{n_1, n_2, n_3\}$ where k and $\{n_1, n_2, n_3\}$ are the wavenumber in the wave propagation direction and the directional cosines.

In the treated case of wave propagation, the sagittal plane is always perpendicular to an even-order symmetry axis of a crystal. Coupled equations (17) of motion describe propagation of "pure" waves, according to Ref. [6, 7]. Hence, the coupled equations of motion can be readily written in the following simplified form, leaving only equations for waves with polarization perpendicular to the sagittal plane and non-zero components of the material tensors:

$$\rho\frac{\partial^2 U_2}{\partial t^2} = C_{44}\left(\frac{\partial^2 U_2}{\partial x_1^2} + \frac{\partial^2 U_2}{\partial x_3^2}\right) + e_{16}\frac{\partial^2 \varphi}{\partial x_1^2} + e_{14}\frac{\partial^2 \varphi}{\partial x_1 \partial x_3} + e_{36}\frac{\partial^2 \varphi}{\partial x_3 \partial x_1} + e_{34}\frac{\partial^2 \varphi}{\partial x_3^2}$$

$$0 = e_{16}\frac{\partial^2 U_2}{\partial x_1^2} + e_{14}\frac{\partial^2 U_2}{\partial x_1 \partial x_3} + e_{36}\frac{\partial^2 U_2}{\partial x_3 \partial x_1} + e_{34}\frac{\partial^2 U_2}{\partial x_3^2} - \varepsilon_{11}\left(\frac{\partial^2 \varphi}{\partial x_1^2} + \frac{\partial^2 \varphi}{\partial x_3^2}\right) \qquad (19)$$

where the single mechanical displacement component U_2 is directed along the x_2-axis in figure 1:

$$U_2 = U_2^0 \exp\left[\mathrm{j}k\left(n_1 x_1 + n_3 x_3 - V_{ph} t\right)\right]$$

$$\varphi = \varphi^0 \exp\left[\mathrm{j}k\left(n_1 x_1 + n_3 x_3 - V_{ph} t\right)\right] \qquad (20)$$

In equation (20), the phase velocity V_{ph} is defined as follows: $V_{ph} = \omega/k$.

Substituting the mechanical displacement U_2 and electrical potential φ of equation (20) into equations (19) of motion, the equations of motion can be readily written in the well-known tensor form, using corresponding components of the well-known Green-Christoffel equation [6, 7]: GL_{22}, $\mathrm{GL}_{42} = \mathrm{GL}_{24}$ and GL_{44}. That gives the following system of two homogeneous equations, using $n_3 = k_3/k$:

$$\begin{pmatrix} \mathrm{GL}_{22} - C_{44}(V_{ph}/V_{t4})^2 & \mathrm{GL}_{24} \\ \mathrm{GL}_{42} & \mathrm{GL}_{44} \end{pmatrix}\begin{pmatrix} U_2^0 \\ \varphi^0 \end{pmatrix} = \begin{pmatrix} 0 \\ 0 \end{pmatrix} \qquad (21)$$

where

$$\mathrm{GL}_{22} = C_{44}(1+n_3^2)$$

$$\mathrm{GL}_{24} = \mathrm{GL}_{42} = e_{16} + (e_{14}+e_{36})n_3 + e_{34}n_3^2$$

$$\mathrm{GL}_{44} = -\varepsilon_{11}(1+n_3^2) \tag{22}$$

In equations (21) and (22), the directional cosines are defined as follows: $n_1 \equiv 1$, $n_2 \equiv 0$ and $n_3 = n_3$. The parameter $V_{t4} = (C_{44}/\rho)^{1/2}$ represents the speed of the bulk SH-wave in some particular cases. Setting the determinant of the coefficient matrix in equations (21) equal to zero, a suitable V_{ph} satisfying boundary conditions written in the following sections and four polynomial roots $n_3^{(p)}(V_{ph})$ can be determined, with which the unknown U_2^0 and φ^0 can be also determined as functions of the V_{ph}. For example, they can be written in the following form, using equations (21) and (22):

$$\varphi^0 = \mathrm{GL}_{42} \text{ and } U_2^0 = -\mathrm{GL}_{44} \tag{23}$$

Expanding the determinant of matrix in equation (22), the secular equation is written as follows:

$$(1+K_1^2)n_3^4 + K_2^2 n_3^3 + (1+A_t^2+K_3^2)n_3^2 + K_4^2 n_3 + (K^2 + A_t^2) = 0 \tag{24}$$

where there are the following non-dimensional values:

$$A_t^2 = 1-\left(V_{ph}/V_{t4}\right)^2$$

$$K^2 = e_{16}^2/(C_{44}\varepsilon_{11})$$

$$K_1^2 = e_{34}^2/(C_{44}\varepsilon_{11})$$

$$K_2^2 = 2e_{34}(e_{14}+e_{36})/(C_{44}\varepsilon_{11})$$

$$K_3^2 = [(e_{14}+e_{36})^2 + 2e_{16}e_{34}]/(C_{44}\varepsilon_{11})$$

$$K_4^2 = 2e_{16}(e_{14}+e_{36})/(C_{44}\varepsilon_{11})$$

Note that K^2 is called the static coefficient of electromechanical coupling (CEMC). Equation (24) represents the fourth order polynomial for which there is a very complicated procedure to determine its roots n_3. Therefore, the polynomial roots are usually determined numerically. Notwithstanding, it is possible to treat some particular cases listed in table 1 in order to significantly simplify the problem for analytical investigations. Note that the following equalities $e_{16} = -e_{34}$ and $e_{14} = e_{36}$ always occur as shown in figure 2.

The first case in table 1 concerning propagation direction [100] was treated in Ref. [11], where the following equality $e_{16} = e_{34} = 0$ (hence $K^2 = K_1^2 = K_2^2 = K_4^2 = 0$) gives $GL_{24} = GL_{42} = 2en_3$ with $e = e_{14} = e_{36}$ and all completely imaginary roots of equation (24) for $V_{ph} < V_t$. This is true for case 5 in propagation direction [001] and the last case in the table. However, case 5 for negative piezoelectric constants $e = e_{14} = e_{36}$ gives the same n_3 and negative $GL_{24} = GL_{42} = -2en_3$ resulting in negative φ^0 in equation (23). Hence, the electrical field E in equation (9) will change its sign. In these cases, the speed V_t of the bulk SH-wave is equal to the V_{t4}. This indicates that these waves in propagation direction [100] are not coupled with the electrical potential. It is clearly seen from the last term of equation (24) that in any other treated case the bulk velocity V_t is equal to the following:

$$V_t = V_{t4}(1 + K^2)^{1/2} \tag{25}$$

The second particular case listed in table 1 is more complicated than the first and can be studied numerically for comparison with the other cases. That is very interesting, because here there is an equality of absolute values of all piezoelectric constants giving $GL_{24} = GL_{42} = e(-1 + 2n_3 + n_3^2)$. Therefore, other analogical cases 4, 6, and 8 in table 1 can be also studied numerically.

Some evaluations for the third case in table 1 concerning propagation direction [101] can be readily done analytically making substitution in equation (24) such as $m_3 = 1 + n_3^2$ and using the piezoelectric constants $e_{16} = -e_{34}$ and $e_{14} = e_{36} = 0$, which give $GL_{24} = GL_{42} = e(-1 + n_3^2)$ for the case. For case 7 in the table there is $GL_{24} = GL_{42} =$

$e(1 - n_3^2)$ that changes the electrical-field sign similarly to cases 1 and 5 discussed above. As the result of such transformations, the equation (24) is written in the following simplified form:

$$(1+K^2)m_3^2 - Bm_3 + 4K^2 = 0 \text{ with } B = \left(\frac{V_{ph}}{V_{t4}}\right)^2 + 4K^2 \tag{26}$$

of which two roots are as follows:

$$m_3^{(1,2)} = \frac{B \pm \sqrt{B^2 - 16K^2(1+K^2)}}{2(1+K^2)} \tag{27}$$

giving the following four polynomial roots of equation (24)

$$n_3^{(1,2,3,4)} = \pm\sqrt{-1 + m_3^{(1,2)}} \tag{28}$$

Table 1. The piezoelectric constants $e_{14} = e_{36}$, e_{16}, and e_{34} [C/m^2] in some highly-symmetric propagation directions for the cubic crystal $Bi_{12}SiO_{20}$

Case	Direction	Degree	$e_{14} = e_{36}$	e_{16}	e_{34}
1.	[100]	0^o	1.122	0.0	0.0
2.	–	~ 22.5^o	0.793	– 0.793	0.793
3.	[101]	45^o	0.0	– 1.122	1.122
4.	–	~ 67.5^o	– 0.793	– 0.793	0.793
5.	[001]	90^o	– 1.122	0.0	0.0
6.	–	~ 112.5^o	– 0.793	0.793	– 0.793
7.	[$\bar{1}$01]	135^o	0.0	1.122	– 1.122
8.	–	~ 157.5^o	0.793	0.793	– 0.793
9.	[$\bar{1}$00]	180^o	1.122	0.0	0.0

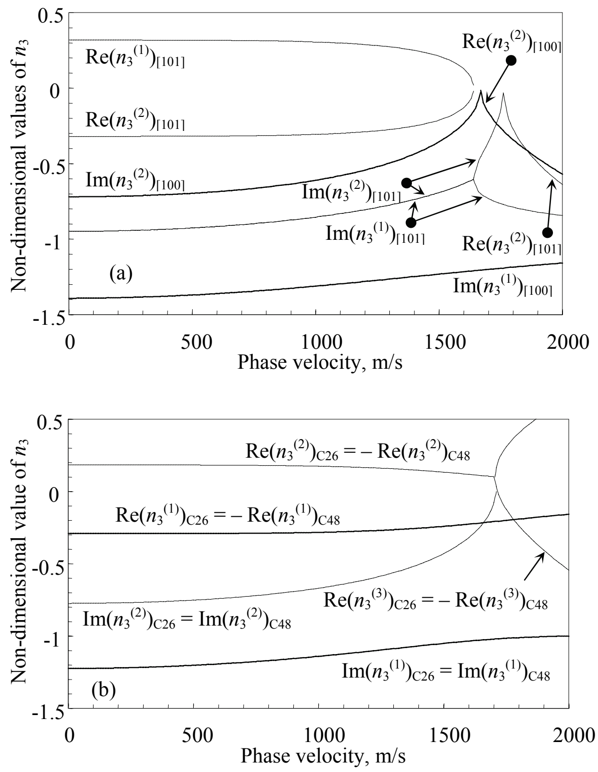

Figure 3. The n_3 real and imaginary parts along the x_3-axis for the propagation directions listed in table 1: (a) cases 1, 3, 5, 7, and 9 for $Bi_{12}GeO_{20}$; (b) cases 2, 4, 6, and 8 with the corresponding subscripts “C26” and “C48” for $Bi_{12}GeO_{20}$

The polynomial roots $n_3^{(1,2,3,4)}$, representing eigenvalues, are shown in figure 3 for the cases listed in table 1. Each eigenvalue n_3 has its own eigenvector $\{U_2^0, \varphi^0\}$ in equation (23) shown in figure 4. Figure 3a compares eigenvalues for cases 1 and 3 listed in table 1. It is clearly seen that the eigenvalues for direction [100] are completely imaginary or real, while they can be complex for direction [101]. As the result, the eigenvectors corresponding to direction [100] are completely imaginary or real, but they can be complex for direction [101] as shown in figure 4a.

Also, it is clearly seen in figure 3 that absolute values of all n_3 imaginary parts begin to decrease with increase in V_{ph} starting at $V_{ph} = 0$. It is well-known that the SAW penetration depth depends on values of Im(n_3). For comparison, purely imaginary roots for cases 2, 4, 6, and 8 listed in table 1 cannot exist that is clearly seen in figure 3b. That statement can be significant in order to choose crystal cuts for finding SAWs. Each eigenvalue n_3 shown in figure 3b possesses its own eigenvector, of which the real and imaginary parts are drawn in figure 4b.

Further analyzing the roots for propagation direction [101] in equations (27) and (28), it can be found that all complex roots can be calculated, when sign of the expression under square root in equation (27) is negative. This fulfills for velocities V_{ph} being lower some velocity V_{ph0} obtained solving the following equation:

$$B^2 - 16K^2\left(1 + K^2\right) = 0 \tag{29}$$

The velocity V_{ph0} is defined by the following formula:

$$V_{ph0} = a_K V_{t4} \text{ with } a_K = 2\sqrt{K\sqrt{1+K^2} - K^2} \tag{30}$$

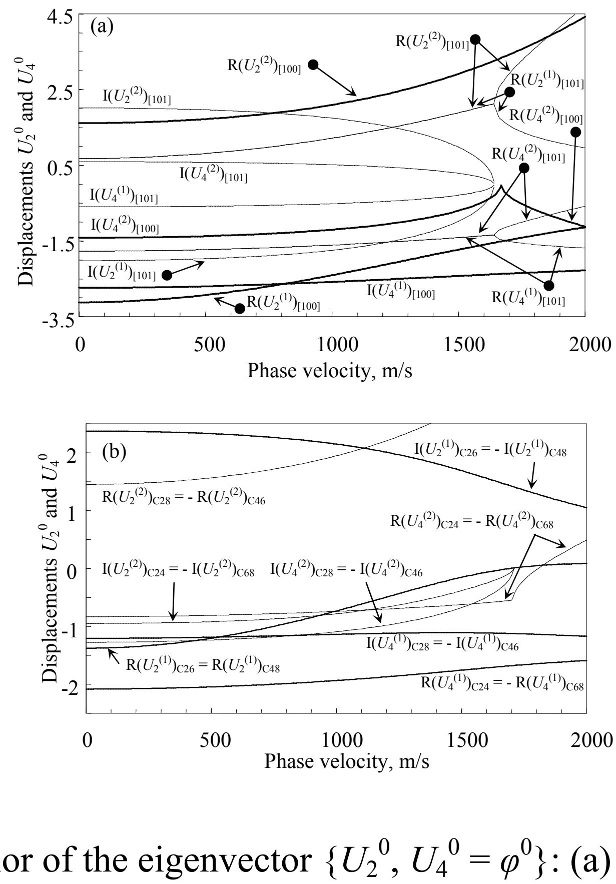

Figure 4. The behavior of the eigenvector $\{U_2^0, U_4^0 = \varphi^0\}$: (a) propagation directions [100] (bold lines) and [101] (thin lines) for $Bi_{12}GeO_{20}$; (b) cases 2, 4, 6, and 8 with the corresponding subscripts such as "C26", etc., for $Bi_{12}GeO_{20}$

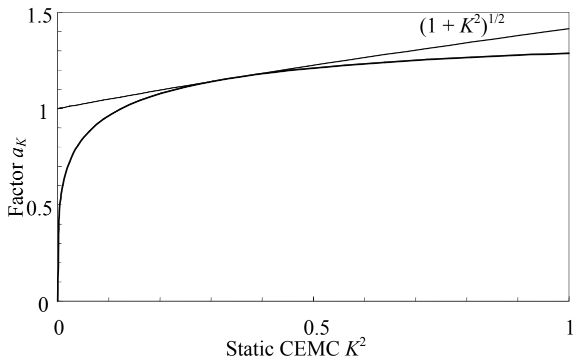

Figure 5. The dependence of the non-dimensional factor a_K on the non-dimensional value of static CEMC K^2. The function $(1 + K^2)^{1/2}$ is shown for comparison

It is clearly seen in equation (30) that the factor a_K is a function of the CEMC K^2 shown in figure 5 together with the other function $f(K^2) = (1 + K^2)^{1/2}$ from equation (25). It is clearly seen in figure 5 that about $K_0^2 = 1/3$ the function $a_K(K^2)$ approaches the function $f(K^2) = (1 + K^2)^{1/2}$ giving the following equality: $V_{ph0} = V_t$. Hence, only complex polynomial roots can exist for $V_{ph} < V_{ph0}$. The CEMC $K_0^2 = 1/3$ is readily calculated by substituting the velocity V_t from equation (25) instead of the V_{ph} in equation (29). However, the form of polynomial roots depends on the K^2: for $K^2 < K_0^2$ there are all imaginary roots for $V_{ph} > V_{ph0}$, but a large $K^2 > K^2_0$ gives real roots for $V_{ph} > V_{ph0}$. Note that formula (30) represents the velocity V_{ph0}, at which the complex roots become completely imaginary for $K^2 < K_0^2$. Moreover, the absolute values of all four imaginary roots are equal to each other giving the solution V_{ph0}. Indeed, two equal negative imaginary roots give the same set of eigenvector components. As a consequence, the boundary-condition determinant written in the following section will become equal to zero. Note that only complex/imaginary roots with negative imaginary parts are chosen in order to have wave damping towards depth of a crystal corresponding to negative values of the x_3-axis shown in figure 1. For comparison, table 2 lists characteristics for some weak piezoelectrics with the cubic symmetry.

Table 2. The characteristics of piezoelectric cubic crystals of class $\bar{4}3m$. The material constants C_{44}, e_{14}, ε_{11}, and ρ are written here following those in Ref. [25]. The velocity $V_{ph0} = a_K V_{t4}$ was calculated using equation (30) for propagation direction [101]. The used ZnTe dielectric constant ε_{11} was announced in Ref. [26]. Noted that the SAW velocity V_{SAW} listed in this table for the weak piezoelectrics differs from the Bleustein-Gulyaev wave velocity calculated with the following well-known formula: $V_{BG} = V_t\{1 - (K^2/[(1 + K^2)\times(1 + \varepsilon_{11}/\varepsilon_0)])^2\}^{1/2}$ where $\varepsilon_0 = 0.08854\times10^{-10}$ [F/m]. Some of the weak piezoelectrics were also studied in Refs. [39-42]

Crystal	C_{44}, 10^{10} N/m^2	e_{14}, C/m^2	ε_{11}, 10^{-10} F/m	ρ, kg/m^3	K^2, %
GaAs	**5.940**	**– 0.160**	**1.107**	**5316**	**0.389319**
GaP	**6.260**	**– 0.100**	**0.983**	**4301**	**0.162507**
β-ZnS	**4.613**	**0.147**	**0.735**	**4091**	**0.637329**
ZnSe	**3.920**	**0.049**	**0.779**	**5264**	**0.078626**
InSb	**3.040**	**0.080**	**1.549**	**5790**	**0.135911**
ZnTe	**3.120**	**0.0284**	**0.894**	**5636**	**0.028916**
$Bi_4(GeO_4)_3$	**4.360**	**0.0376**	**1.417**	**7120**	**0.022883**
$Bi_4(SiO_4)_3$	**5.180**	**0.0830**	**1.434**	**6800**	**0.092742**
Crystal	**a_K**	**V_{t4}, m/s**	**V_t, m/s**	**V_{SAW}, m/s**	**V_{ph0}, m/s**
GaAs	**0.484246**	**3342.725669**	**3349.226288**	**3349.226145**	**1618.702294**
GaP	**0.393547**	**3815.069424**	**3818.168042**	**3818.168010**	**1501.409546**
β-ZnS	**0.543005**	**3357.971359**	**3368.655030**	**3368.654232**	**1823.395247**
ZnSe	**0.330243**	**2728.884115**	**2729.956717**	**2729.956707**	**901.195778**
InSb	**0.376999**	**2291.382067**	**2292.938660**	**2292.938653**	**863.848699**
ZnTe	**0.258597**	**2352.836803**	**2353.176957**	**2353.176955**	**608.436933**
$Bi_4(GeO_4)_3$	**0.244132**	**2474.589967**	**2474.873085181**	**2474.873085**	**604.127170**
$Bi_4(SiO_4)_3$	**0.343746**	**2760.008525**	**2761.288076**	**2761.288069**	**948.741383**

However, it is commonly thought that it is necessary to account the piezoelectric effect only for strong piezoelectric crystals with $K^2 > 1\%$. The interesting feature of cubic crystals with a weak piezoelectric effect is a slow velocity V_{ph0} in equation (30), depending on both V_{t4} and a_K. In general, values of the factor a_K are confined between 0.2 and 0.5 for piezoelectrics of class $\bar{4}3$m, and a small value of V_{t4} (for example, $V_{t4}(Tl_3TaS_4) \sim 687$ m/s and $V_{t4}(Tl_3TaSe_4) \sim 751$ m/s [25]) can give a slow V_{ph0}. Hence, using the factor a_K of formula (30) and figure 3, one can examine that the penetration depth in weak piezoelectrics with the cubic symmetry can be comparable with that in stronger ones. Note that the V_{ph0} for cubic piezoelectrics with $K^2 < 1/3$ must be experimentally verified, because it has "latent" characteristics. In addition to table 2, the strong piezoelectrics of class 23 have the following CEMCs: $K^2(Bi_{12}SiO_{20}) \sim 0.141$ and $K^2(Bi_{12}GeO_{20}) \sim 0.113$.

Note that the SAWs cannot be found in cubic crystals with a large $K^2 > 1/3$ in the V_{ph}-range: $V_{ph0} < V_{ph} < V_t$. That can manifest a strong instability of such piezoelectric crystals concerning SH-SAW propagation. Here, there are all complex roots for $V_{ph} < V_{ph0}$, all real roots for $V_{ph0} < V_{ph} < V_t$, and one pair of complex conjugated roots with two real roots for $V_{ph} > V_t$. It is thought that a large K^2 can be observed in complex compounds, as well as in simple ones including cubic piezoelectrics. For instance, the classic ferroelectric $PbTiO_3$ has been known to have a single ferroelectric tetragonal (T) to paraelectric cubic phase transition with increased temperature or pressure. Results of Ref. [27] studying $PbTiO_3$ discuss an unexpected tetragonal-to-monoclinic-to-rhombohedral-to-cubic phase transition sequence induced by hydrostatic pressure and a morphotropic phase boundary in a pure compound. In the transition regions, $PbTiO_3$ can possess huge dielectric and piezoelectric coupling constants similar to those observed in the new complex single-crystal solid-solution piezoelectrics $Pb(Mg_{1/3}Nb_{2/3})O_3$-$PbTiO_3$ (PMN-PT) and $Pb(Zn_{1/3}Nb_{2/3})O_3$-$PbTiO_3$ (PZN-PT) which are expected to revolutionize electromechanical applications. The complex piezoelectrics, for instance, the most widely used piezoelectric material $PbZrO_3$-$PbTiO_3$ (PZT), being ubiquitous in modern technology, have piezoelectric coefficients an order of magnitude larger than those of conventional ferroelectric simple compounds [28]. In addition, Ref. [27] suggests that the giant piezoelectric effect can be studied in simple systems, because this effect as well as the morphotropic phase boundary effect does not require intrinsic disorder.

CHAPTER III. Boundary Conditions for SH-waves in Monocrystals

Boundary conditions studying SH-waves in monocrystals ($h = 0$ in figure 1) are based on several requirements which must be satisfied. There is the single mechanical boundary condition on the normal component of the stress tensor τ_{32} at $x_3 = 0$ ($\tau_{32} = 0$) where

$$\tau_{32} = \sum_{p=1,2} F^{(p)} \left[C_{44} k_3^{(p)} U_2^{(p)} + (e_{14} k_1 + e_{34} k_3^{(p)}) \phi^{(p)} \right] \tag{31}$$

There are two electrical boundary conditions: continuity of the normal component D_3 of the electrical displacements at $x_3 = 0$, namely at the interface between a vacuum (D_3^f) and the crystal surface, where

$$D_3 = \sum_{p=1,2} F^{(p)} \left[(e_{36} k_1 + e_{34} k_3^{(p)}) U_2^{(p)} - \varepsilon_{33} k_3^{(p)} \phi^{(p)} \right]$$

$$D_3^f = -F^{(0)} \phi_0^f \mathrm{j} k_1 \varepsilon_0 \tag{32}$$

and continuity of the electrical potential ϕ at $x_3 = 0$ ($\phi = \phi^f$) where

$$\phi = \sum_{p=1,2} F^{(p)} \phi^{(p)} \text{ and } \phi^f = F^{(0)} \phi_0^f \tag{33}$$

Therefore, the third-order boundary-condition determinant (BCD3) of a matrix can be readily formed from equations (31) – (33), using the weight functions $F^{(0)}$, $F^{(1)}$, and $F^{(2)}$ as unknown factors. It is noted that BCD3 can be readily reduced to BCD2 for finding the V_{ph}, because values of the electrical potential ϕ and the electrical displacement component D_3 can be taken to be not independent, for example, see Refs. [6, 7, 29]. Once ϕ is given, a fixed value of D_3 is also given. Therefore, two electrical boundary conditions (32) and (33) at the free surface can be written as follows:

$$D_3 = \sum_{p=1,2} F^{(p)} \left[(e_{36}k_1 + e_{34}k_3^{(p)})U_2^{(p)} - (\varepsilon_{33}k_3^{(p)} - \mathrm{j}k_1\varepsilon_0)\phi^{(p)} \right] \qquad (34)$$

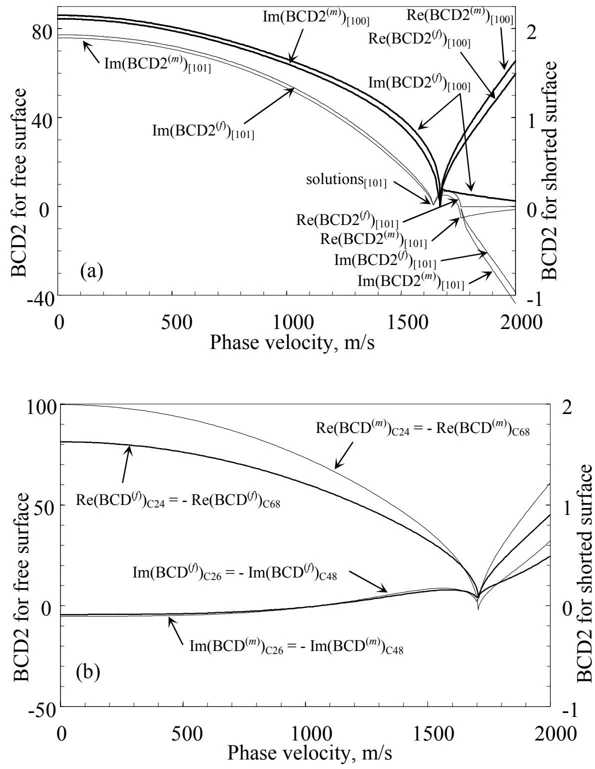

Figure 6. The behavior of the non-dimensional value of determinant BCD2 using the material constants of $Bi_{12}GeO_{20}$: (a) propagation directions [100] and [101] of cases 1 and 3 listed in table 1; (b) cases 2, 4, 6, and 8 of table 1. Different electrical boundary conditions of free surface (see "*f*") and surface metallization ("*m*") are shown

Figure 6 shows behavior of the determinants corresponding to the cases listed in table 1 for different electrical boundary conditions of free surface and surface metallization. Figure 6a compares the BCD2 behavior of cases 1, 3, and relevant listed in table 1 with more complicated cases 2, 4, 6, and 8 shown in figure 6b. It is clearly seen that the BCD2 for direction [101] equals to zero at the velocity V_{ph0}. Figure 7 shows the velocity V_t of the bulk acoustic wave (BAW) using different crystal cuts for both $Bi_{12}SiO_{20}$ and $Bi_{12}GeO_{20}$ as well as the found solutions V_{ph0} in direction [101].

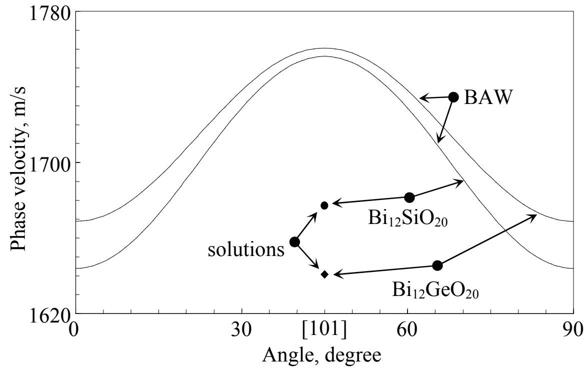

Figure 7. The speeds V_t of the bulk SH-waves in dependence on the propagation directions from [100] to [001] for cubic piezoelectric crystals $Bi_{12}SiO_{20}$ and $Bi_{12}GeO_{20}$

The complete mechanical displacement U_2^{Σ} and electrical potential φ^{Σ} are written in the plane wave form as follows, using suitable eigenvalues and eigenvectors of obtained V_{ph}:

$$U_2^{\Sigma} = \sum_{p=1,2} F^{(p)} U_2^{0(p)} \exp\left[jk\left(n_1 x_1 + n_3^{(p)} x_3 - V_{ph} t\right)\right]$$

$$\varphi^{\Sigma} = \sum_{p=1,2} F^{(p)} \varphi^{0(p)} \exp\left[jk\left(n_1 x_1 + n_3^{(p)} x_3 - V_{ph} t\right)\right] \tag{35}$$

The weight functions $F^{(1)}$ and $F^{(2)}$ are readily determined from equation (34) and show the following relationship:

$$F^{(1)} = -F^{(2)} \tag{36}$$

because two equal eigenvalues $n_3^{(1)} = n_3^{(2)}$ give the same eigenvectors $\{U_2^{0(1)}, \varphi^{0(1)}\}$ and $\{U_2^{0(2)}, \varphi^{0(2)}\}$.

It is obvious that the weight factors $F^{(1)} = -F^{(2)}$ in equation (36) will zero the complete mechanical displacement U_2^{Σ} and electrical potential φ^{Σ} in equation (35). That means that the V_{ph0} solution in equation (30) is always obtained and represents a "latent" possibility concerning SAW existence in piezoelectric cubic monocrystals, supplementing the opinion of Gulyaev written in Ref. [10]. Hence, there is a possibility to change boundary conditions that can be achieved by a mass loading in order to apply some additional perturbation to the surface of a cubic crystal for finding SAWs. Therefore, the following sections relate to studying dispersive SAWs in various layered structures consisting of cubic piezoelectrics.

CHAPTER IV. Boundary Conditions for SH-waves in Layered Systems

Mass loading such as with a thin film on the free surface of a monocrystal significantly complicates the problem of finding SAWs, and one deals here with the layered system shown in figure 1. Therefore, boundary conditions for SH-waves must be written for two sides of the layer: the layer-substrate interface at $x_3 = 0$ (see figure 1) and the layer-vacuum interface at $x_3 = h$. It is obvious that equality of the mechanical displacements U_2 along the x_2-axis must be at $x_3 = 0$ ($U_2^S = U_2^L$) where

$$U_2^S = \sum_{S(p)} F^{S(p)} U_2^{S(p)} \text{ and } U_2^L = \sum_{L(p)} F^{L(p)} U_2^{L(p)} \qquad (37)$$

Here the superscripts S and L are for the substrate and layer, respectively. The second condition on the stress tensor normal component τ_{32} at $x_3 = 0$ requires continuity resulting in $\tau_{32}{}^S = \tau_{32}{}^L$, where

$$\tau_{32}^S = \sum_{S(p)} F^{S(p)} \left[C_{44}^S k_3^{S(p)} U_2^{S(p)} + (e_{14}^S k_1 + e_{34}^S k_3^{S(p)}) \phi^{S(p)} \right]$$
$$\tau_{32}^L = \sum_{L(p)} F^{L(p)} \left[C_{44}^L k_3^{L(p)} U_2^{L(p)} + (e_{14}^L k_1 + e_{34}^L k_3^{L(p)}) \phi^{L(p)} \right] \qquad (38)$$

Two electrical boundary conditions at $x_3 = 0$ require continuity of the normal component D_3 of the electrical displacements ($D_3{}^s = D_3{}^l$) where

$$D_3^S = \sum_{S(p)} F^{S(p)} \left[(e_{36}^S k_1 + e_{34}^S k_3^{S(p)}) U_2^{S(p)} - \varepsilon_{33}^S k_3^{S(p)} \phi^{S(p)} \right]$$
$$D_3^L = \sum_{L(p)} F^{L(p)} \left[(e_{36}^L k_1 + e_{34}^L k_3^{L(p)}) U_2^{L(p)} - \varepsilon_{33}^L k_3^{L(p)} \phi^{L(p)} \right] \qquad (39)$$

as well as continuity of the electrical potential ϕ ($\phi^S = \phi^L$) where

$$\phi^S = \sum_{S(p)} F^{S(p)} \phi^{S(p)} \text{ and } \phi^L = \sum_{L(p)} F^{L(p)} \phi^{L(p)} \tag{40}$$

At the free surface $x_3 = h$ there is a single mechanical boundary condition $\tau_{31}{}^L = 0$, where

$$\tau_{32}^L = \sum_{L(p)} F^{L(p)} \left[C_{44}^L k_3^{L(p)} U_2^{L(p)} + (e_{14}^L k_1 + e_{34}^L k_3^{L(p)}) \phi^{L(p)} \right] \times \exp\left(\mathrm{j} k_3^{L(p)} h \right) \tag{41}$$

as well as one electrical boundary condition, according to Ref. [29]:

$$D_3^{Lf} = \sum_{L(p)} F^{L(p)} \left[(e_{36}^L k_1 + e_{34}^L k_3^{L(p)}) U_2^{L(p)} - (\varepsilon_{33}^L k_3^{L(p)} - \mathrm{j} k_1 \varepsilon_0) \phi^{L(p)} \right] \times \exp\left(\mathrm{j} k_3^{L(p)} h \right) \tag{42}$$

In equations (37) – (42), the index p runs from 1 to 2 for the substrate and from 1 to 4 for the layer.

The boundary-condition determinant can be readily formed using equations (37) – (42), which will be used for finding SH-SAWs. Such SAWs propagate in the layer by damping towards the substrate depth. Also, SAW propagation in piezoelectrics can be coupled with the electrical potential, which can be found in a vacuum and keeps all information about the propagating SAWs. It is thought that the electrical potential amplitude should decrease in a vacuum from the layer free surface. Accounting all partial displacement components $F^{S(p)}$ in the substrate and electrical one $F^{(0)}$ in a vacuum in addition to the components $F^{L(p)}$ for the layer, the resulting waves will be seven-partial. Therefore, the studied boundary-condition determinant (BCD) will be called below seven-order BCD7.

Structures consisting of a layer on a substrate have an additional parameter such as the layer thickness h complicating theoretical investigations of wave existence. Therefore, it is natural to choose a constant value of h. The non-dimensional value of kh is commonly used, where k is the wavenumber in wave propagation direction. Various propagation directions and various layered systems are analyzed in figure 8 for the same value of $kh = 1$, using the strong piezoelectric cubic crystals $Bi_{12}SiO_{20}$

and $Bi_{12}GeO_{20}$. Note that the bulk SH-wave speed for $Bi_{12}SiO_{20}$ is lower than that for $Bi_{12}GeO_{20}$. For instance, in direction [101], they are as follows: $V_t^S = V_t(Bi_{12}SiO_{20}) \sim$ 1756.104 m/s and $V_t^G = V_t(Bi_{12}GeO_{20}) \sim$ 1760.575 m/s.

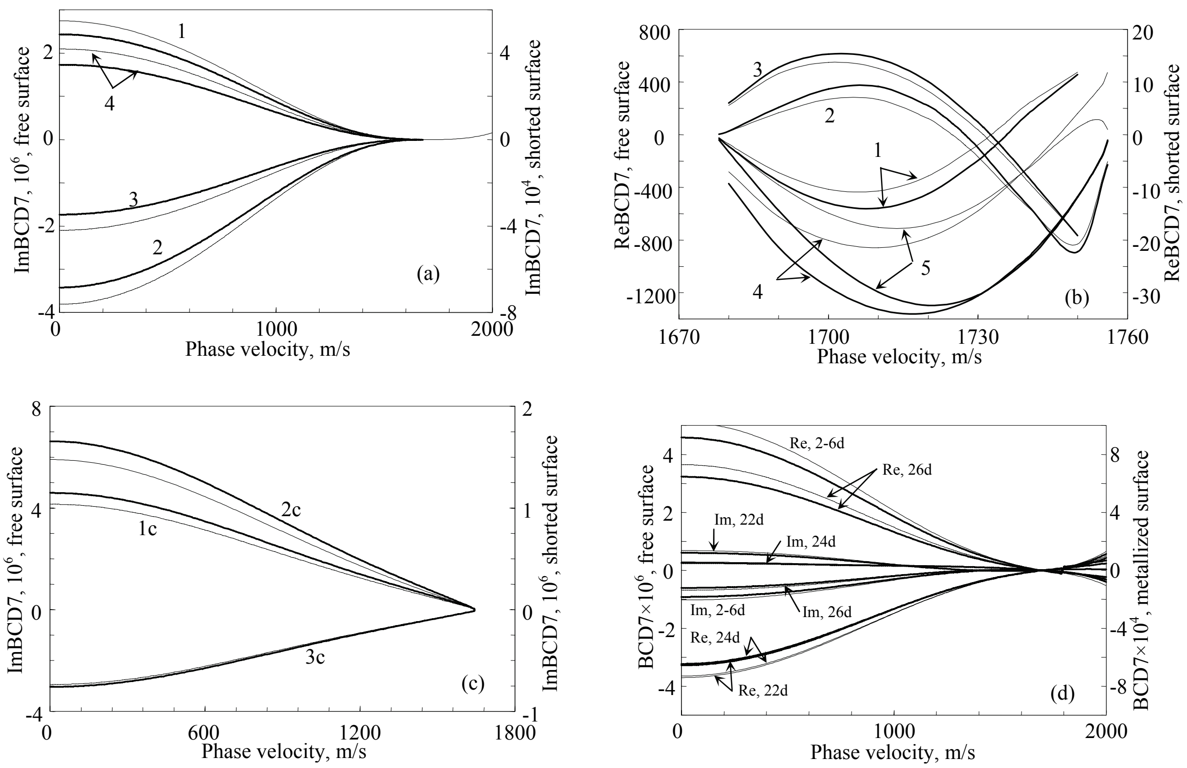

Figure 8. The comparison of BCD7 behaviors in dependence on the V_{ph} at $kh = 1$ for the cases of free surface (thick lines) and surface metallization (thin lines). (a) Propagation direction [101]: "1", "2", "3", "4", and "5" label the layered systems such as the layer of $Bi_{12}SiO_{20}$(case 7 in table 1) on the substrate of $Bi_{12}GeO_{20}$(case 3 in table 1), $Bi_{12}SiO_{20}$(3)/$Bi_{12}SiO_{20}$(7), $Bi_{12}GeO_{20}$(3)/$Bi_{12}SiO_{20}$(7), $Bi_{12}GeO_{20}$(3)/$Bi_{12}SiO_{20}$(3), and $Bi_{12}SiO_{20}$(3)/$Bi_{12}GeO_{20}$(3), respectively, which are the same for (b) showing V_{ph}-range $V_{ph0} < V_{ph} < V_t$ for purely imaginary roots in direction [101]; (c) propagation direction [100] with "1c", "2c", and "3c" being for the layered systems $Bi_{12}SiO_{20}$(1)/$Bi_{12}GeO_{20}$(5), $Bi_{12}SiO_{20}$(1)/$Bi_{12}SiO_{20}$(5), and $Bi_{12}GeO_{20}$(5)/$Bi_{12}SiO_{20}$(1); (d) combinations of the other cases listed in table 1: "22d", "24d", "26d", and "2-6d" are for the structures $Bi_{12}SiO_{20}$(2)/$Bi_{12}GeO_{20}$(2), $Bi_{12}SiO_{20}$(2)/$Bi_{12}GeO_{20}$(4), $Bi_{12}SiO_{20}$(2)/$Bi_{12}GeO_{20}$(6), and $Bi_{12}SiO_{20}$(2)/$Bi_{12}SiO_{20}$(6)

It is possible to suggest that some surface waves can be found possessing the $V_{ph} < V_t^S$ because $V_t^S < V_t^G$. Concerning propagation direction [101] in the layered systems shown in figures 8a and 8b, some solutions of BCD7 can be obtained for different electrical boundary conditions (free surface and surface metallization) only in the V_{ph}-range: $V_{ph0} < V_{ph} < V_t^S$. The solutions correspond to new dispersive SH-SAWs, because surface Bleustein-Gulyaev wave cannot exist in piezoelectric cubic crystals. The interesting case is the layered systems consisting of the $Bi_{12}SiO_{20}$-layer on the $Bi_{12}SiO_{20}$-substrate with different polarities (cases 3 and 7 in table 1) in which the new dispersive SH-SAWs can be also found. It is thought that this situation can be found as a defect of crystal growth.

The following section discusses dispersion relations for the new SH-SAWs propagating in direction [101] of various layered structures. It is clearly seen in figures 8a, 8c, and 8d that the BCD7 has large values for small V_{ph} in all possible layered systems, and possible solutions can be obtained only when the V_{ph} approaches the speed V_t of bulk SH-wave. However, any solutions of surface waves were not revealed when the propagation direction corresponds to direction [100] for both the cubic crystals, for which the BCD7 behaviors are shown in figure 8c. The same negative result was obtained for the propagation directions and layered systems shown in figure 8d. Indeed, for the other cases 2, 4, 6, and 8 listed in table 1, the real and imaginary parts of complex BCD7 shown in figure 8d change their sign at different V_{ph} for all possible structures consisting of the studied cubic crystals. Also, an existence possibility of dispersive SAWs, using propagation directions [101] and [100] for a layer and substrate, respectively, was not verified assuming that these two-layer structures are more complicated. Such investigations can be readily carried out in the future by the same method analyzing BCD7 behaviors, if such problems will be highlighted for possible applications.

CHAPTER V. Numerical Results and Discussions

It is thought that dispersion relations representing dependencies $V_{ph}(kh)$ are the most impotent characteristic of dispersive waves. It is obvious that the problem of finding of SH-waves in layered systems, using an additional parameter such as the layer thickness h, is richer concerning possible obtained results. Figure 9 – showing dispersion relations for SH-waves propagating in piezoelectric cubic crystals – supports such statement, because it is thought that the new dispersive SH-SAWs can be observed in an array of various layered systems.

Figure 9a introduces results for several layered systems with the $Bi_{12}SiO_{20}$-substrate, whereas figure 9b introduces additional results for two possible configurations with the $Bi_{12}GeO_{20}$-substrate. SH-waves propagate in direction [101] or relevant (see cases 3 and 7 in table 1) for both a layer and substrate in all the cases, using the electrical boundary conditions of free and shorted surfaces to receive more information about the new dispersive waves.

It is clearly seen in figures 9a and 9b that the new SH-SAWs possess the single mode in each case with the following condition for the phase velocity V_{ph} < $V_t(Bi_{12}SiO_{20})$ < $V_t(Bi_{12}GeO_{20})$. Also, such peculiarities as the non-dispersive Zakharenko waves [30] corresponding to all the extreme points of the phase velocity V_{ph} versus the non-dimensional value of kh are clearly seen in figure 9. Therefore, the existence of such type of the non-dispersive waves at these points in suitable layered structures allows utilization of the structures instead of monocrystals in different SAW technical devices. This was also discussed in Ref. [30]. Note that two extreme points of the function $V_{ph}(kh)$ can be found in figure 9. This is similar to the in-plane-polarized Rayleigh type waves studied in Ref. [31], in which two non-dispersive Zakharenko type waves can be also found.

Using the $Bi_{12}SiO_{20}$-substrate, the following layered systems in figure 9a can be discussed:

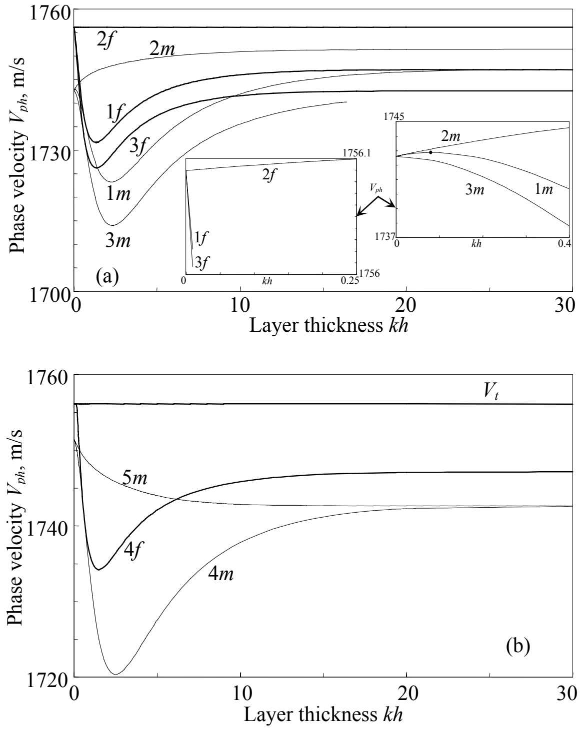

Figure 9. The dispersion relations in various layered systems consisting of the cubic crystals $Bi_{12}SiO_{20}$ and $Bi_{12}GeO_{20}$. (a) The $Bi_{12}SiO_{20}$-substrate was used: "1*f*", "2*f*", and "3*f*" are for the case of free surface and the layered systems $Bi_{12}GeO_{20}$(case 7 in table 1)/$Bi_{12}SiO_{20}$(case 3 in table 1), $Bi_{12}GeO_{20}$(3)/$Bi_{12}SiO_{20}$(3), and $Bi_{12}SiO_{20}$(7)/$Bi_{12}SiO_{20}$(3), respectively; "1*m*", "2*m*", and "3*m*" are for the case of surface metallization and the corresponding layered systems. The left and right insertions show the mode beginnings with the single point denoting the first non-dispersive Zakharenko wave. (b) The $Bi_{12}GeO_{20}$-substrate was used: "4*f*" and "4*m*" are for the layered system $Bi_{12}SiO_{20}$(3)/$Bi_{12}GeO_{20}$(7), and "5*m*" is for $Bi_{12}SiO_{20}$(3)/$Bi_{12}GeO_{20}$(3). The non-dispersive Zakharenko waves correspond to extreme points of the function $V_{ph}(kh)$

1) The first structure consists of the $Bi_{12}GeO_{20}$-layer rotated according to case 7 in table 1 on the $Bi_{12}SiO_{20}$-substrate using case 3 in the table. Here, the V_{ph} for the free-surface electrical condition starts with the SAW velocity $V_{ph}^{f0}(Bi_{12}SiO_{20})$ ~

1756.0896 m/s [32, 37] < $V_t(Bi_{12}SiO_{20})$ ~ 1756.104 m/s, comes to the minimum value of ~ 1731.650 m/s at kh ~ 1.336, and approaches the non-dispersive interfacial-wave velocity ~ 1747.138 m/s [37] for a large value of kh ($kh \to \infty$). However, the different V_{ph}-behavior occurs for the shorted-case mode, which begins with the velocity $V_{ph}^{m0}(Bi_{12}SiO_{20})$ ~ 1742.609 m/s [32, 37] at zero kh and approaches the same value of ~ 1747.138 m/s [37] for $kh \to \infty$. The V_{ph} has the maximum value of ~ 1742.870 m/s at small kh ~ 0.08 shown by the point in the right insertion in figure 9a and the minimum value of ~ 1723.242 m/s at kh ~ 2.26. It is thought that all the V_{ph} extreme points can be readily found in experiments by a method based on sign evaluation of the derivative dV_{ph}/dkh. This was also discussed in Ref. [18].

2) For the $Bi_{12}GeO_{20}(3)/Bi_{12}SiO_{20}(3)$ structure, the free-surface case V_{ph} originating with the V_{ph}^{f0} at zero kh increases and reaches $V_t(Bi_{12}SiO_{20})$ at kh ~ 0.27. This is shown in the left insertion in figure 9a. The same qualitative behavior occurs for the shorted-case mode, which originates with the SAW velocity $V_{ph}^{m0}(Bi_{12}SiO_{20})$ ~ 1742.609 m/s [32, 37] at kh = 0 and increases to the SAW velocity V_{ph}^{m1} $(Bi_{12}GeO_{20})$ ~ 1751.469 m/s [32, 37].

3) Probably, the most interesting configuration is $Bi_{12}SiO_{20}(7)/Bi_{12}SiO_{20}(3)$, in which the same material is used for both the layer and substrate applying two possible polarities (possible defect of crystal growth). Indeed, here there occurs the open-surface mode beginning with the velocity V_{ph}^{f0} at kh = 0, and the V_{ph} achieves the velocity V_{ph}^{m0} for $kh \to \infty$. The minimum V_{ph} has the value of ~ 1726.235 m/s at kh ~ 1.37. It is natural that the metallized-surface mode also starts with the velocity V_{ph}^{m0} at zero kh. Notwithstanding, it does not return to the V_{ph}^{m0} interrupting at kh ~ 16.379. The minimum V_{ph}-value for this interrupted mode is ~ 1713.989 m/s at kh ~ 2.32.

The following reverse configurations with the $Bi_{12}GeO_{20}$-substrate shown in figure 9b can be also analyzed:

4) For the $Bi_{12}SiO_{20}(3)/Bi_{12}GeO_{20}(7)$ configuration with V_t(layer) < V_t(substrate), the free-surface mode in figure 9b commences with $V_{ph} = V_t(Bi_{12}SiO_{20})$ at $kh \sim 0.159$, but not at zero kh. That gives the "silence" kh-zone for the waves. With increase in kh, the V_{ph} runs through the minimum value of ~ 1734.207 m/s at $kh \sim 1.49$. For large values of $kh > 30$, the V_{ph} approaches the interfacial-wave velocity ~ 1747.138 m/s [37] also calculated for the $Bi_{12}GeO_{20}(7)/Bi_{12}SiO_{20}(3)$ structure. The shorted-surface mode originates with $V_{ph}(kh = 0) = V_{ph}^{m1}$ and, going through the minimum value of ~ 1720.372 m/s at $kh \sim 2.5$, returns up to the velocity V_{ph}^{m0} for $kh \to \infty$.

5) A free-surface mode does not exist for the $Bi_{12}SiO_{20}(3)/Bi_{12}GeO_{20}(3)$ configuration. However, the single mode for the shorted-surface case begins with the velocity V_{ph}^{m1} at zero kh and decreases to the velocity V_{ph}^{m0} for $kh \to \infty$. Note that the mode behavior is reverse to that for the reverse configuration: $Bi_{12}GeO_{20}(3)/Bi_{12}SiO_{20}(3)$.

It is thought that the $Bi_{12}GeO_{20}(3)/Bi_{12}GeO_{20}(7)$ structure will have similar dispersion relations obtained for the $Bi_{12}GeO_{20}(3)/Bi_{12}GeO_{20}(7)$ structure. Concerning the studied different structures, it is obvious that each structure is unique that can be useful in defectoscopy of grown crystals and interface inspection of two-layer structures.

For comparison, Ref. [9] particularly discusses a similar case when the layer and the substrate are identical $LiNbO_3$ of class 3 m, except that they are polarized in opposite directions. Here, the phase velocities V_{f0} and V_{s0} for the surface electrically free and shorted conditions, respectively, were also obtained when the layer is in the absence of initial stresses. In Ref. [9], dispersive BG-waves were calculated in the layered piezoelectric $LiNbO_3$-structure possessing a single mode. Their results show that for a given value of kh, the phase velocity of the free-surface case is higher than that of electrically shorted case. Also, in the limit of $kh \to 0$ the wave mode tends to the surface BG-wave in a piezoelectric half-space with the phase velocities $V_{f0} \sim 4538$ m/s for the free-surface case and $V_{s0} \sim 4203$ m/s for the shorted-surface condition.

With increasing the value of kh from zero, the velocities V_{f0} and V_{s0} rapidly decrease to their minimum V_{ph}-values corresponding to the non-dispersive Zakharenko type waves. With increasing the value of kh to 3, the velocities V_{f0} and V_{s0} asymptotically tend to 4202 m/s.

The non-dispersive Zakharenko waves [30], representing extreme points of the function $V_{ph}(kh)$ in dispersion relations for dispersive waves, can be described by the following formulas, using the following formula $\mathrm{d}(u/v)/\mathrm{d}x = (v\mathrm{d}u/\mathrm{d}x - u\mathrm{d}v/\mathrm{d}x)/v^2$ which is well-known as Leibniz's formula:

$$\frac{\mathrm{d}V_{ph}}{\mathrm{d}kh} = V_g \frac{\mathrm{d}V_{ph}}{\mathrm{d}\omega h} = 0 \tag{43}$$

$$\frac{\mathrm{d}V_{ph}}{\mathrm{d}kh} = \frac{1}{kh}\left(V_g - V_{ph}\right) \tag{44}$$

$$\frac{\mathrm{d}V_{ph}}{\mathrm{d}\omega h} = \frac{V_{ph}}{\omega h}\left(1 - \frac{V_{ph}}{V_g}\right) \tag{45}$$

The relationship (43) between the V_{ph}-derivatives shows that there is independence of the V_{ph} on both the angular frequency ω and the wavenumber k in the same k-ω-domain with $V_g \neq 0$. The formulas (44) and (45) clarify that formula (43) is satisfied when the phase and group velocities are equal in dispersion relations for the wavenumber $k \neq 0$ and $k < \infty$. It is thought that the case of $V_g = V_{ph} \to 0$ ($V_g = V_{ph} = 0$) represents the Bose-Einstein condensation (BEC). It is possible to show that for the BEC near zero, the following relationship $V_g \sim 2V_{ph}$ ($V_g = 2V_{ph}$) occurs for a free quasi-particle propagating in a vacuum. Therefore, the BEC as dispersive waves can correspond to inflection points of both the V_g and V_{ph}.

It is possible to evaluate the coefficient of electromechanical coupling (CEMC) K_c^2 of the new dispersive SH-SAWs for some interesting layered systems, for which the dispersion relations are shown in figure 9. For the $Bi_{12}SiO_{20}$(7)/$Bi_{12}SiO_{20}$(3) structure with different polarities shown in figure 10, the K_c^2 approaches the maximum value of ~ 2% at kh ~ 4 to 5. Note that the $Bi_{12}SiO_{20}$(7)/$Bi_{12}SiO_{20}$(3) and $Bi_{12}SiO_{20}$(3)/$Bi_{12}SiO_{20}$(7) structures show the same dispersion relations, and therefore, the same dependencies $K_c^2(kh)$. It is also noted that the K_c^2 is interrupted for the structures at K_{c0}^2 (kh_c ~ 16.378) ~ 0.27% due to the mode interruption at kh_c for the case of surface metallization. When the $Bi_{12}SiO_{20}$-layer is substituted by the $Bi_{12}GeO_{20}$-layer with the same polarity to form the structure $Bi_{12}GeO_{20}$(7)/$Bi_{12}SiO_{20}$(3) with $V_t(Bi_{12}GeO_{20}) > V_t(Bi_{12}SiO_{20})$, the K_c^2 has the maximum value slightly larger than 1.43% and smaller than $K_c^2(kh \to 0)$ ~ 1.54%, and approaches zero already at kh = 30. This can manifest that the new dispersive SH-SAWs at large values of $kh > 30$ behave as waves propagating in non-piezoelectric crystals with zero K_c^2. This occurs as soon as the V_{ph} for the case reaches the interfacial-wave velocity V_{in1} ~ 1747.138 m/s [37] which is unique for the structure. The value of V_{in1} is significantly larger than both values of $V_t^{[100]}(Bi_{12}SiO_{20})$ ~ 1643 m/s and $V_t^{[100]}(Bi_{12}GeO_{20})$ ~ 1668 m/s. Omitting the piezoelectric effect in the calculations for direction [101], one can also find that $V_t^{[101]} = V_t^{[100]}$.

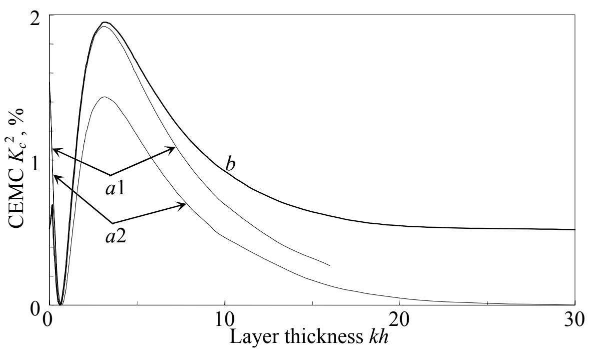

Figure 10. The coefficient of electromechanical coupling (CEMC) K_c^2 (%) calculated with formula (46) for the layered systems such as $Bi_{12}SiO_{20}$(case 7 in table 1)/$Bi_{12}SiO_{20}$(case 3 in table 1), $Bi_{12}GeO_{20}$(7)/$Bi_{12}SiO_{20}$(3), and $Bi_{12}SiO_{20}$(3)/$Bi_{12}GeO_{20}$(7) denoted by "a1", "a2", and "b", respectively

However, treating the reverse configuration to $Bi_{12}SiO_{20}$(3)/$Bi_{12}GeO_{20}$(7), namely when the $Bi_{12}SiO_{20}$-substrate is substituted by the $Bi_{12}GeO_{20}$-one to form the $Bi_{12}SiO_{20}$(3)/$Bi_{12}SiO_{20}$(7) structure, the K_c^2 also achieves the maximum value of ~ 2% at kh ~ 4 to 5. In this $Bi_{12}SiO_{20}$(3)/$Bi_{12}GeO_{20}$(7) structure in which several modes of Love type waves can also exist from kh = 0 to kh = 200, the K_c^2 approaches some relatively small value of 0.5% for a large value of kh > 30 (see figure 10). That indicates some coupling with the electrical potential and can be used in addition to the modes of the Love waves. It is clearly seen in the figure that in these three calculated cases, the K_c^2 equals to zero at $kh \sim 0.5$ to 0.7.

The CEMC shown in figure 10 was calculated for the single modes of the new dispersive SH-SAWs with the following well-known formula:

$$K_c^2 = 2\frac{V_f - V_m}{V_f} \tag{46}$$

where V_f and V_m are the velocities for the free and metallized surfaces, respectively. It is noted that the K_c^2 for the other configurations shown in figure 9 was not calculated, because the velocities for the cases of free surface are equal to the speed V_t^S = $V_t(Bi_{12}SiO_{20})$ or are slightly below V_t^S at small values of kh. That can mean disappearance of SAW dispersive modes. Note that characteristics of the new non-dispersive SAW propagating in the monocrystals such as $Bi_{12}SiO_{20}$ and $Bi_{12}SiO_{20}$ were investigated in Ref. [32].

The layered structures, consisting of piezoelectric cubic crystals GaP and GaAs, can be readily fabricated, for example, see the work [33] on properties of interface and relaxation properties of grown GaP/GaAs structures by chemical beam epitaxy. The production technology of the structures is continuously improved. The crystals are widely used to fabricate multi-layered structures such as photonic crystals and superlattices. It is thought that they are also suitable for study of a possible existence of the new dispersive SAWs propagating in layered structures like GaP/GaAs. Also, it is noted that GaAs is used as a substrate material, for instance, in the layered structure ZnO/GaAs [34], which are currently of a great interest for design of integrated SAW filters. Indeed, GaP can be also used as a substrate material. In addition to thin films made from hexagonal ZnO and cubic ZnS possessing low toxicity and being inexpensive and easily obtained, thin films made from the cubic crystal ZnTe (see table 2) can be also used in layered structures for various applications. Also, these materials have continuously attracted attention as potentially useful active optoelectronic materials.

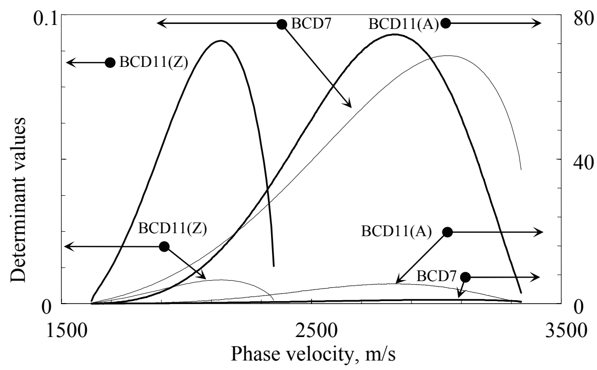

Figure 11. The Re(BCD11) behavior for the multi-layered structures GaAs/GaP/GaAs (see "A") and ZnTe/GaP/GaAs (see "Z") in dependence on the V_{ph}, using both electrical boundary conditions of free surface (thick lines) and surface metallization (thin lines). Here there is V_{ph0}(GaP) < V_{ph} < V_t(GaAs) for GaAs/GaP/GaAs and V_{ph0}(GaP) < V_{ph} < V_t(ZnTe) for ZnTe/GaP/GaAs (see table 2). The following parameters were set: $kh = 1$, $h_1/h = 1$ and $h_2/h = 3$ where h_1 is the layer thickness for the first layer (GaP) and h_2 is the one for the second layer (GaAs or ZnTe). For comparison, the Re(BCD7) behavior for the GaP/GaAs structure with kh = 1 is also shown

Therefore, any existence of the new dispersive SAWs was verified in such layered systems as GaP/GaAs, GaAs/GaP, ZnTe/GaAs, and GaAs/ZnTe. It is thought that the new dispersive SAWs cannot be found in such layered systems and in some multi-layered structures (see figure 11) consisting of the weak piezoelectrics. Note that for some layered structures consisting of the weak piezoelectrics listed in table 2, the velocity V_{SAW} listed in the table is also found for very small values of $kh \sim 10^{-5}$. Notwithstanding, these SAW solutions cannot be found already at $kh \sim 10^{-4}$. Also, it is possible to investigate the new SAW existence in layered systems consisting of non-cubic crystals by studying suitable propagation directions, in which the surface Bleustein-Gulyaev waves cannot exist. Ref. [35] discusses some cases when the surface BG-waves cannot exist in crystals of hexagonal class 622 and tetragonal class 422. Therefore, theoretical investigations concerning non-cubic crystals can be reported in the future.

CHAPTER VI. Love Type Waves

Concerning the existence of the seven-partial Love type waves (LTW7) propagating in the configuration of the $Bi_{12}SiO_{20}$-layer on the $Bi_{12}GeO_{20}$-substrate, the LTW7 several modes are shown in figure 12 for two possible cases such as normal polarity for $Bi_{12}SiO_{20}(3)/Bi_{12}GeO_{20}(3)$ and different polarity for $Bi_{12}SiO_{20}(3)/Bi_{12}GeO_{20}(7)$, using different electrical boundary conditions. It was found that the first non-shorted-case LTW7-mode for $Bi_{12}SiO_{20}(3)/Bi_{12}GeO_{20}(3)$ begins with some velocity $V_1 \sim 1760.565$ m/s slightly lower than the speed $V_t(Bi_{12}GeO_{20}) \sim 1760.575$ m/s. Note that the velocity difference $\Delta V = V_t - V_1 \sim 10$ mm/s is significant, because the calculation accuracy was set about 1 μm/s. It is thought that the unshorted-case LTW7-modes for $Bi_{12}SiO_{20}(3)/Bi_{12}GeO_{20}(7)$ start with the second mode as shown in figure 12, and the first mode looks like it can only start outside the positive values of *kh*. This can mean that it does not exist similar to the first shorted-case LTW7-modes for both the $Bi_{12}SiO_{20}(3)/Bi_{12}GeO_{20}(3)$ and $Bi_{12}SiO_{20}(3)/Bi_{12}GeO_{20}(7)$ structures. The beginnings of the all existing modes in the *kh*-range $0 < kh < 200$ are listed in table 3. It is clearly seen in the table that the higher-order mode beginnings for $Bi_{12}SiO_{20}(3)/Bi_{12}GeO_{20}(7)$, starting with the second modes of shorted and non-shorted cases, are shifted towards the smaller values of *kh* with the constant *kh*-step such as $kh_s \sim 12$ relative to the corresponding those for $Bi_{12}SiO_{20}(3)/Bi_{12}GeO_{20}(3)$.

It is also obvious, using both figure 12 and table 3, that a shorted-case mode starts at a smaller value of *kh* in comparison with a corresponding original *kh*-value of non-shorted-case mode providing the usual relationship $V_{s1}/V_{f1} < 1$. Here, V_{s1} and V_{f1} are the velocities for shorted and non-shorted cases at the same suitable value of kh_1, at which both modes exist. This indicates that all the LTW7 modes are very sensitive to an external perturbation applied to the free surface, which is widely used for sensor applications. It is also noted that the unusual behavior of the LTW7 lowest-order mode of the shorted case is shown by the empty points in figure 12 for

$Bi_{12}SiO_{20}$(3)/$Bi_{12}GeO_{20}$(7). The mode starts with the velocity V_t($Bi_{12}GeO_{20}$) at some kh_0 ~ 9.61 and achieves the bulk SH-wave velocity V_t($Bi_{12}SiO_{20}$) already at kh ~ 11.7.

Table 3. The *kh*-positions of mode beginning for various layered systems

Mode number	**$Bi_{12}SiO_{20}$(3)/ $Bi_{12}GeO_{20}$(3), free surface**	**$Bi_{12}SiO_{20}$(3)/ $Bi_{12}GeO_{20}$(3), metallized surface**	**$Bi_{12}SiO_{20}$(3)/ $Bi_{12}GeO_{20}$(7), free surface**	**$Bi_{12}SiO_{20}$(3)/ $Bi_{12}GeO_{20}$(7), metallized surface**
1	0.0	-	-	-
2	30.88	21.63	18.88	9.61
3	62.30	53.05	50.30	41.05
4	93.72	84.47	81.72	72.47
5	125.14	115.89	113.14	103.89
6	156.56	147.31	144.56	135.31
7	187.98	178.73	175.98	166.73

It is also possible to discuss that a large *kh*-"silence" zone occurs for both the electrical boundary conditions in the $Bi_{12}SiO_{20}$(3)/$Bi_{12}GeO_{20}$(7) structure, see figure 12. It is natural that for very large values of *kh*, the first mode of the unshorted case and all the higher-order modes of the treated cases approach the speed V_t($Bi_{12}SiO_{20}$) ~ 1756.104 m/s. It was also found that each following mode is equally distant from the corresponding previous mode with the *kh*-step: kh_{s0} ~ 31.42, excluding the unusual modes such as the first mode starting at kh = 0 and the shorted-case mode starting at kh_0 ~ 9.61 for the $Bi_{12}SiO_{20}$(3)/$Bi_{12}GeO_{20}$(7) structure listed in table 3. For comparison, the paper [36] by Kessenikh *et al.* discusses LTW7 propagation in layered systems, consisting of an isotropic layer on a transversely-isotropic substrate of classes 6, 4, 6 mm, 4 mm, 622, and 422. In Ref. [36], they introduced the dynamic CEMC K_D^2 depending on the non-dimensional value of *kh*. They also discussed the possible cases when the K_D^2 sign is positive or negative, as well as when the K_D^2 sign is changed at some critical *kh* with increase in the value of *kh*. Applying their theoretical results to the studied layered systems in this paper, it is possible to discuss that the K_D^2 is different for the $Bi_{12}SiO_{20}$(3)/$Bi_{12}GeO_{20}$(3) and $Bi_{12}SiO_{20}$(3)/$Bi_{12}GeO_{20}$(7) structures, because the first non-shorted LTW7-mode for $Bi_{12}SiO_{20}$(3)/$Bi_{12}GeO_{20}$(3) begins with $V_1 < V_t$($Bi_{12}GeO_{20}$) and, because there is the *kh*-“silence” zone for the LTW7 propagating in the $Bi_{12}SiO_{20}$(3)/$Bi_{12}GeO_{20}$(7) structure. Note that the “silence” zone also occurs for the new SH-SAWs propagating in the $Bi_{12}SiO_{20}$(3)/$Bi_{12}GeO_{20}$(7) structures.

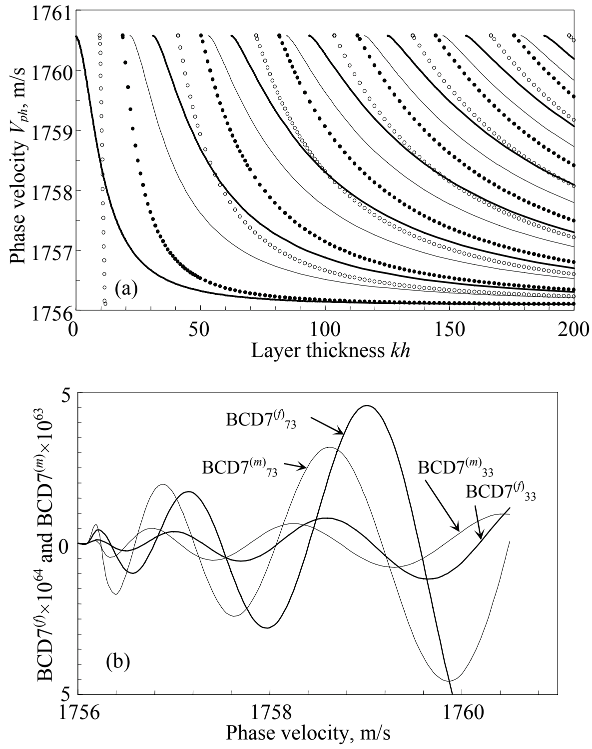

Figure 12. (a) The LTW7 several modes. The thick and thin lines represent the cases of free and metallized surfaces, respectively, for the layered systems consisting of the layer of $Bi_{12}SiO_{20}$ (case 3 in table 1) on the substrate of $Bi_{12}GeO_{20}$ (case 3 in table 1). The filled and empty cycles represent the cases of free and metallized surfaces for $Bi_{12}SiO_{20}$(3)/$Bi_{12}GeO_{20}$(7). (b) The boundary-condition determinants (BCD7) at kh = 200: “*f*” and “*m*” are for the free and metallized surfaces, and “33” and “73” are for the layered systems $Bi_{12}SiO_{20}$(3)/$Bi_{12}GeO_{20}$(3) and $Bi_{12}SiO_{20}$(7)/$Bi_{12}GeO_{20}$(3)

CONCLUSION

These theoretical investigations of SH-SAW existence in piezoelectric cubic crystals when the SAWs propagate in direction [101] perpendicular to an even-order symmetry axis of a piezoelectrics demonstrated the following results:

the surface Bleustein-Gulyaev waves cannot exist in piezoelectric cubic monocrystals that confirms Gulyaev's statement recently written in Ref. [10]. Indeed, the new surface SH-waves called the ultrasonic surface Zakharenko waves (USZWs) can propagate in cubic piezoelectrics [32] and cubic piezomagnetics [38], which differ from the surface Bleustein-Gulyaev waves;

the new dispersive SH-SAWs can be found in various layered structures consisting of a layer on a substrate, for instance, in strong piezoelectrics such as $Bi_{12}SiO_{20}$ and $Bi_{12}GeO_{20}$;

it is thought that such dispersive SH-SAWs cannot be solidly revealed in the layer-on-substrate structures using weakly-piezoelectric cubic crystals such as GaAs, GaP, and ZnTe. The existence of the new SH-SAW was also verified by studying multi-layered structures consisting of the weak piezoelectrics: GaAs/GaP/GaAs and GaAs/GaP/ZnTe.

Also, surface SH-waves propagating in direction [100] were not found studying various layer-on-substrate structures consisting of $Bi_{12}SiO_{20}$ and $Bi_{12}GeO_{20}$, as well as in the other directions listed in table 1 for both materials. This indicates that propagation direction [101] is unique concerning the new SH-SAW existence, using different electrical boundary conditions of free surface and surface metallization for strong piezoelectric cubic crystals.

The seven-partial Love type wave (LTW7) can also exist in the $Bi_{12}SiO_{20}/Bi_{12}GeO_{20}$ layered system with $V_t(Bi_{12}GeO_{20}) > V_t(Bi_{12}SiO_{20})$ and in the same structures with the other possible polarity at the layer-substrate interface. It is thought that the polarity phenomenon as an interfacial defect can be readily distinguished in manufactured layered structures. Also, it was found that the LTW7 mode beginnings for the neighbour modes are equidistant from each other. It was also found that the LTW7 phase velocity is very sensitive to any change in the crystal polarity (different electrical boundary conditions). This can be used for filter and sensor applications.

The theoretical investigations of the two-layer systems described in this work can be also applied to layered systems consisting of cubic piezomagnetics, because piezoelectrics and piezomagnetics can be described in the same way following Ref. [43]. However, the magnetoelectrical effect must be accounted when a piezoelectrics and a piezomagnetics are used to create piezoelectric/piezomagnetic laminated composites. Some works on the subject are cited in Refs. [43-57]. It is also worth noting that the recent book in Ref. [57] acquaints theoreticians and experimentalists with several new hear-horizontal surface acoustics waves (SH-SAWs) in piezoelectromagnetics of class 6 mm.

ACKNOWLEDGEMENTS

The author is grateful to all the Referees for useful notes. Also, the author is grateful to the LAP LAMBERT Academic Publishing GmbH & Co. KG for the granted right to publish this manuscript with the LAP.

REFERENCES

[1] Lord Rayleigh (J.W. Strutt) "On waves propagated along the plane surfaces of an elastic solid" *Proceedings of the London Mathematical Society* **17** 4 – 11 (1885).

[2] A.E.H. Love, *Some problems of Geodynamics*, Cambridge University Press, London (England), 1911.

[3] J.L. Bleustein, "A new surface wave in piezoelectric materials" *Applied Physics Letters* **13** 412 – 413 (1968).

[4] Yu.V. Gulyaev, "Electroacoustic surface waves in solids" *Soviet Physics Journal of Experimental and Theoretical Physics Letters* **9** 37 – 38 (1969).

[5] G.W. Farnell, Types and properties of surface acoustical waves, in: A.A. Oliner (Ed.), *Acoustic Surface Waves*, **Vol. 24**, Springer Verlag, Berlin–Heidelberg–New York, 1978, pp. 26 – 109.

[6] C. Lardat, C. Maerfeld, P. Tournois, "Theory and performance of acoustical dispersive surface wave delay lines" *Proceedings of the IEEE* **59** (3) 355 – 364 (1971).

[7] G.W. Farnell, E.L. Adler, Elastic wave propagation in thin layers, in: W.P. Mason and R.N. Thurston (Eds.), *Physical Acoustics*, **Vol. 9,** Academic Press, New York, 1972, pp. 35 – 127.

[8] E. Dieulesaint, D. Royer, *Elastic waves in solids: applications to signal processing*/ translated by A. Bastin and M. Motz, Chichester [English]; New York, J. Wiley, 1980, 511 pages.

[9] H. Liu, Z.B. Kuang, Z.M. Cai, "Propagation of Bleustein-Gulyaev waves in a prestressed layered piezoelectric structures" *Ultrasonics* **41** 397 – 405 (2003).

[10] Yu.V. Gulyaev, F.S. Hickernell, "Acoustoelectronics: history, present state and new ideas for a new Era" *Acoustical Physics Reports* (Akusticheskii Zhurnal, Moscow) **51** (1) 101 – 110 (2005), in Russian.

[11] A.A. Zakharenko, "Love type waves in layered systems consisting of two piezoelectric cubic crystals" *Journal of Sound and Vibration* **285** (4–5) 877 – 886 (2005).

[12] M.I. Kaganov, I.L. Sklovskaya, "On surface waves in piezoelectrics" *Soviet Physics of Solid State* (Moscow) **8** (12) 3480 – 3483 (1966), in Russian.

[13] V.I. Al'shits, V.N. Lyubimov, "Two types of special bulk waves in piezoelectrics and existence sectors of Bleustein–Gulyaev waves" *Soviet Kristallografiya* (Crystallography Reports, Moscow) **30** (3) 437 – 444 (1985), in Russian.

[14] C.C. Homes, T. Vogt, S.M. Shapiro, S. Wakimoto, M.A. Subramanian, A.P. Ramirez, "Charge transfer in the high dielectric constant materials $CaCu_3Ti_4O_{12}$ and $CdCu_3Ti_4O_{12}$" *Physical Review B* **67** 092106 (2003) 12 pages.

[15] M. Yamaguchi, "Early days of SH–type surface acoustic wave research" *Japanese Journal of Applied Physics* **42**, Part 1, N° 5B, 2909 – 2917 (2003).

[16] Yu.V. Gulyaev, "Review of shear surface acoustic waves in solids" *IEEE Transactions on Ultrasonics, Ferroelectrics, and Frequency Control* **45** (4) 935 – 938 (1998).

[17] S.V. Biryukov, Yu.V. Gulyaev, V.V. Krylov, V.P. Plessky, *Surface Acoustic Waves in Inhomogeneous Media*, L.M. Brekhovskikh (Edr.), Springer Series on Wave Phenomena, **Vol. 20**, Springer-Verlag, Berlin-Heidelberg-New York, 1995, 388 pages.

[18] A.A. Zakharenko, "Analytical studying the group velocity of three-partial Love (type) waves in both isotropic and anisotropic media" *Non-destructive Testing and Evaluation* **20** (4) 237 – 254 (2005).

[19] W.G. Cady, "Piezoelectricity", McGraw Hill, New York, 1946, 359 pages.

[20] W.P. Mason, "Applications of acoustical phenomena" *Journal of Acoustical Society of America* **68** (1) 53 – 63 (1980).

[21] W.P. Mason, "Piezoelectricity, its history and applications" *Journal of Acoustical Society of America* **70** (6) 1561 – 1566 (1981).

[22] D.A. Berlincourt, D.R. Curran, H. Jaffe, “Piezoelectric and piezomagnetic materials and their function in transducers”, in *Physical Acoustics: Principles and Methods*, edited by W.P. Mason, **Vol. 1**, Part A, Academic Press, New York, 1964, pages 169 – 270.

[23] V.E. Lyamov, *Polarization effects and interaction anisotropy of acoustic waves in crystals*, Moscow, MSU Publishing, 1983, 224 pages.

[24] J.F. Nye, *Physical Properties of Crystals. Their representation by tensors and matrices*, Oxford at the Clarendon Press, 1989, 385 pages.

[25] A.A. Blistanov, V.S. Bondarenko, N.V. Perelomova, F.N. Strizhevskaya, V.V. Chkalova, M.P. Shaskol’skaya, Acoustical Crystals, in: M.P. Shaskol’skaya (Ed.), *Acoustical Crystals*, Nauka, Moscow, 1982, 632 pages (in Russian).

[26] T. Yamamoto, “Control of N-impurity states in N-doped ZnO, ZnS, and ZnTe” *Japanese Journal of Applied Physics* **42** (Part 2, No. 5B) L514 – L516 (2003).

[27] Zh. Wu, R.E. Cohen, “Pressure-induced anomalous phase transitions and colossal enhancement of piezoelectricity in $PbTiO_3$” *Physical Review Letters* **95** 037601 (2005), 4 pages.

[28] S.-E. Park, T.R. Shrout, “Ultrahigh strain and piezoelectric behavior in relaxor based ferroelectric single crystals” *Journal of Applied Physics* **82** (4) 1804 – 1811 (1997).

[29] K.A. Ingebrigtsen, “Surface waves in piezoelectrics” *Journal of Applied Physics* **40** (7) 2681 – 2686 (1969).

[30] A.A. Zakharenko, “Dispersive Rayleigh type waves in layered systems consisting of piezoelectric crystals bismuth silicate and bismuth germanate” *Acta Acustica united with Acustica* **91** (4) 708 – 715 (2005).

[31] A.A. Zakharenko, “Acoustic waves with the in-plane polarization in piezoelectric cubic structures” *Canadian Journal of Pure & Applied Sciences* **3** (1) 675 – 690 (2009).

[32] A.A. Zakharenko, “New solutions of shear waves in piezoelectric cubic crystals” *Journal of Zhejiang University SCIENCE A* **8** (4) 669 – 674 (2007).

[33] A. Freundlich, A. Bensaoula, A.H. Bensaoula, V. Rossignol, “Interface and relaxation properties of chemical beam epitaxy grown GaP/GaAs structures” *Journal of Vacuum Science and Technology B*: *Microelectronics and Nanometer Structures* **11** (3) 843 – 846 (1993).

[34] V.Y. Zhang, J.E. Lefebvre, T. Gryba, “SAW characteristics in a layered ZnO/GaAs structure for design of integrated SAW filters” *Proceedings of the IEEE Ultrasonic Symposium*, Atlanta, **Vol. 1** 261 – 264 (2001).

[35] G.G. Kessenikh, L.A. Shuvalov, “Transverse surface waves in piezoelectric crystals of classes 622 and 422” *Ferroelectrics* **42** 149 – 152 (1982).

[36] G.G. Kessenikh, V.N. Lyubimov, L.A. Shuvalov, “On surface Love waves in piezoelectrics” *Soviet Kristallografiya* (Crystallography Reports, Moscow) **27** (3) 437–443 (1982), in Russian.

[37] A.A. Zakharenko, “New interfacial shear-horizontal waves in piezoelectric cubic crystals” *Journal of Electromagnetic Analysis and Applications* (Scientific Research Publishing, California, USA) **2** (11) x – x (2010).

[38] A.A. Zakharenko, “First evidence of surface SH-wave propagation in cubic piezomagnetics” *Journal of Electromagnetic Analysis and Applications* (Scientific Research Publishing, California, USA) **2** (5) 287 – 296 (2010).

[39] S.S. Rao, M. Sunar, “Piezoelectricity and its use in disturbance sensing and control of flexible structures: a survey” *Applied Mechanics Review* **47** 113 – 123 (1994).

[40] C.C. Tseng, “Piezoelectric surface waves in cubic crystals” *Journal of Applied Physics* **41** 2270 – 2276 (1970).

[41] G. Koerber, R.F Vogel, “Generalized Bleustein modes”, *The IEEE Transactions on Sonics and Ultrasonics* **SU-19** 3 – 8 (1972).

[42] V.M. Bright, W.D. Hunt, “Bleustein-Gulyaev waves in gallium arsenide and other piezoelectric cubic crystals”, *Journal of Applied Physics* **66** 1556 – 1564 (1989).

[43] V.I. Al’shits, A.N. Darinskii, J. Lothe, “On the existence of surface waves in half-infinite anisotropic elastic media with piezoelectric and piezomagnetic properties” *Wave Motion* **16** (3) 265 – 283 (1992).

[44] J. Ryu, Sh. Priya, K. Uchino, H.-E. Kim, “Magnetoelectric effect in composites of magnetostrictive and piezoelectric materials” *Journal of Electroceramics* **8** 107 – 119 (2002).

[45] M. Fiebig, “Revival of the magnetoelectric effect” *Journal of Physics D: Applied Physics* **38** (8) R123 – R152 (2005).

[46] A.R. Annigeri, N. Ganesan, S. Swarnamani, “Free vibrations of simply supported layered and multiphase magneto-electro-elastic cylindrical shells” *Smart Materials and Structures* **15** 459 – 467 (2006).

[47] J. Aboudi, “Micromechanical analysis of fully coupled electro-magneto-thermo-elastic multiphase composites” *Smart Materials and Structures* **10** 867 – 877 (2001).

[48] P.S. Neelakanta, *Handbook of Electromagnetic Materials*, New York, CRC Press, 1995.

[49] E. Pan, “Three-dimensional Green’s functions in anisotropic magneto-electro-elastic bimaterials” *Zeitschrift der Angewandte Mathematik und Physik* **53** 815 – 838 (2002).

[50] J.Y. Li, “Magnetoelectroelastic multi-inclusion and inhomogeneity problems and their applications in composite materials” *International Journal of Engineering Science* **38** 1993 – 2011 (2000).

[51] B.-L. Wang, Y.-W. Mai, “Applicability of the crack-face electromagnetic boundary conditions for fracture of magnetoelectroelastic materials” *International Journal of Solids and Structures* **44** (2) 387 – 398 (2007).

[52] T.J.-Ch. Liu, Ch.-H. Chue, “On the singularities in a bimaterial magneto-electro-elastic composite wedge under antiplane deformation” *Composite Structures* **72** 254 – 265 (2006).

[53] X.-F. Li, “Dynamic analysis of a cracked magnetoelectroelastic medium under antiplane mechanical and inplane electric and magnetic impacts” *International Journal of Solids and Structures* **42** 3185 – 3205 (2005).

[54] A. Melkumyan, “Twelve shear surface waves guided by clamped/free boundaries in magneto-electro-elastic materials” *International Journal of Solids and Structures* 44 3594 – 3599 (2007).

[55] Y. Huang, X.-F. Li, K.Y. Lee, “Interfacial shear horizontal (SH) waves propagating in a two-phase piezoelectric/piezomagnetic structure with an imperfect interface” *Philosophical Magazine Letters* **89** (2) 95 – 103 (2009).

[56] A.-K. Soh, J.-X. Liu, “Interfacial shear horizontal waves in a piezoelectric-piezomagnetic bi-material” *Philosophical Magazine Letters* **86** (1) 31 – 35 (2006).

[57] A.A. Zakharenko, *Propagation of seven new SH-SAWs in piezoelectromagnetics of class 6 mm*, Saarbruecken – Krasnoyarsk, LAP LAMBERT Academic Publishing GmbH & Co. KG, 76 pages ,2010, ISBN: 978-3-8433-6403-4; This book is available at https://www.morebooks.de/store/gb/book/propagation-of-seven-new-sh-saws-in-piezoelectromagnetics-of-class-6mm/isbn/978-3-8433-6403-4.